

QUANTIFYING TRANSIENT
STORAGE IN REALIGNED AND
NON-REALIGNED RIVER
REACHES.

George Dallow

A thesis submitted in partial fulfilment of the requirements of
Liverpool John Moores University for the degree of Master of
Philosophy

June 2020

Contents

1.0	Abstract.....	4
2.0	Introduction	5
2.1	River Restoration Background	5
2.2	Transient Storage	6
2.3	Measuring Transient Storage.....	7
2.4	Transient Storage Model Limitations.....	9
2.5	Aims and Objectives.....	10
3.0	Methods	11
3.1	Study Site	11
3.1.1	Swindale Beck Location and Catchment.....	11
3.1.2	Swindale Beck Historical Straightening.....	12
3.1.3	Restoration Efforts.....	13
3.2	Tracer Injection Methodology	17
3.3	Modelling Methodology	18
3.3.1	Transient Storage Modelling.....	18
3.3.2	OTIS Model Parameters.....	19
3.3.3	OTIS Transient Storage Parameter Estimates.....	20
3.3.4	Transport Simulations.....	21
3.3.5	Transient Storage Metrics.....	22
3.4	Geomorphic Unit Analysis.....	25
4.0	Results.....	26
4.1	OTIS Model Parameters	26
4.2	Transient Storage Metrics.....	32
4.3	Geomorphic Unit Analysis.....	35
5.0	Discussion.....	40
5.1	Spatial and Temporal Patterns in Transient Storage	40

5.1.1	Damköhler Number	40
5.1.2	FMed@200.....	40
5.1.3	Residence Time in the Transient Storage Zone (TimeStor)	42
5.1.4	Storage Zone Turnover Length (Ls).....	43
5.1.5	Standardised Storage Zone Area (TranStor)	43
5.1.7	Storage Zone Exchange Flux (qs)	43
5.1.8	Hydrologic Retention Factor (Rh)	44
5.2	Summary of Metrics.....	44
5.3	Conceptual Model of Transient Storage	46
5.4	Implications for River Restoration	52
6.0	Conclusions	55
7.0	Acknowledgements.....	57
8.0	References	58
9.0	Appendix	65

1.0 Abstract

Transient storage has been used to quantify catchment-channel interactions, and more recently, as a proxy of ecosystem health in river restoration schemes. However, the impact that river restoration has on transient storage is not well studied. A key area that has not been extensively studied is the effect river restoration has on surface-subsurface interactions, and the evolution of these processes once restoration is completed. This study aims to quantify the effect that river restoration has on transient storage in order to understand how a river responds to restoration efforts and to make recommendations for future restoration schemes. The study site located on the Swindale Beck in Cumbria, UK comprised of three realigned reaches and one non-realigned reach. A conservative salt tracer injection (NaCl) and modelling approach was used to quantify transient storage. Breakthrough curves of the tracer were used in conjunction with the One-Dimensional Transport with Inflow and Storage model, OTIS, to estimate reach hydrodynamic parameters. These parameters were input into the modified OTIS model, OTIS-P, to calculate the transient storage metrics. These metrics were used to quantify transient storage after one month and after one year after restoration. In conjunction with transient storage data, UAV derived photogrammetry of the channel allowed for changes in geomorphological features, channel length, bankfull depth, and width to be quantified. The transient storage metrics describe that residence of channel water time in storage and the length of the storage zone was lower in realigned reaches compared to non-realigned reaches. Storage zone exchange flux and hydrological retention factor show a higher value in the realigned reaches compared to the non-realigned reach. This suggests that the realigned reaches are dominated by rapidly exchanging surface storage, whereas the non-realigned reach was dominated by much slower subsurface storage. A conceptual model is proposed in order to better understand how river restoration affects surface-subsurface exchange within realigned and non-realigned river reaches. It is suggested that the removal of the reinforced banks however, would allow the channel to return to a state of dynamic equilibrium as floodplain access is realigned and natural channel progression can begin to occur.

2.0 Introduction

2.1 River Restoration Background

River restoration is typically undertaken within degraded riverine systems in order to improve geomorphic, hydrologic, and ecologic processes that have been negatively influenced by human activity (Wohl et al., 2005). Restoration may also focus on aesthetic or recreational improvements (Bernhardt and Palmer, 2007) disregarding geomorphic, hydrologic, and ecologic functions. This can be achieved through the reintroduction of removed elements of the natural system and the alteration or removal of compromised components (Beechie et al., 2010, Palmer et al., 2016, Roni et al., 2008, Wohl et al., 2005, Wohl et al., 2015). Common river restoration goals include; bank stabilisation, channel reconfiguration, weir/dam/bridge removal, reconnection of the floodplain, habitat improvement, and species management (Wohl et al., 2015). Typically, a variety of restoration techniques will be used during the restoration of a waterway.

River restoration techniques can be split into two key categories; form-based, and process-based (Wohl et al., 2015). Form-based restoration encourages the alteration of the stream channel in order to improve conditions (Wohl et al., 2015), such as step pools and woody debris introduction, bank stabilisation, and channel reconfiguration. Conversely, process-based restoration focuses on the restoration of the hydrological and geomorphological function. This includes improving lateral (channel to floodplain interactions), longitudinal (along the stream), and vertical (surface-water to ground-water interactions) connectivity, as opposed to focusing primarily on the channel's form (Wohl et al., 2015). Improvements to connectivity can be made through the removal of restrictions such as dams, reinforced banks, and bridges. One of the key advantages of process-based restoration is that the channel is allowed to naturally return to a state of dynamic equilibrium compared to form-based restoration where the channel is designed (potentially incorrectly) for the river (Lave, 2009). Due to the complexity and uniqueness of riverine systems, it is difficult to estimate how long a restoration project will need in order for the water body to reach a pre-degraded state (Bash and Ryan, 2002, Bernhardt et al., 2005). To combat this, form-based and process-based methods may be coupled in order to accelerate the restoration process, as the form-based process

provide short term restoration and the process based restoration ensures the channel improved conditions in the long term (Wohl et al., 2015).

Several studies have found that many river restoration schemes, typically form-based, tend to ignore vertical connectivity, which has been cited as the key failure of many river restoration schemes (Knust and Warwick, 2009, Kurth et al., 2015). Vertical connectivity is an important factor concerning riverine ecosystem sustainability and water quality, as it is the pathway upon which water travels from the surface into the subsurface, and consequently, into the hyporheic zone (Kondolf et al., 2006). It has been shown by Harvey and Bencala (1993) that an increase in hydraulic head gradients and variation in streambed topography and permeability vastly improve vertical connectivity. Installed submerged structures such as boulders and woody debris along with riffles and boulder steps induce areas of downwelling creating a hydraulic head gradient across the feature (Harvey and Bencala, 1993). The hydraulic head facilitates the movement of water into the subsurface and subsequently into the hyporheic zone. This temporary withholding of water within the channel subsurface is known as subsurface storage. In addition to subsurface storage is surface storage zones, this includes: dead-end channels, pools, and wetlands (De Smedt et al., 2005, Ensign and Doyle, 2005, Runkel and Chapra, 1993). This surface and subsurface temporary hydrological retention of river water separate from the main channel is referred to as transient storage (Ensign and Doyle, 2005).

2.2 Transient Storage

The first comprehensive model of transient storage was described by Bencala (1983) and was used extensively to quantify both channel hydrodynamics and processes such as nitrogen, phosphorus, and carbon cycling (Runkel, 2002). The transient storage model consists of two theoretical areas: the main channel and the storage zone. The former is the portion of the stream in which the dominant transport mechanics are advection and dispersion. The latter is the movement of a molecule downstream by the main channel flow, whilst dispersion is related to all constituents within the water flow. The storage zone is defined as the area of the stream that contributes to transient storage (Runkel, 2002), this is an extremely simplified explanation of the storage zone which is not a single entity, but multiple much smaller storage zones (Becker et al., 2013, Choi et al., 2000).

Transient storage includes the exchange of main channel flow with subsurface hyporheic flow and surface water dead zones (Fernald et al., 2001, Gooseff et al., 2003) through a process known as hyporheic exchange. Hyporheic exchange is driven by hydraulic head gradients between a stream and the streambed. The hyporheic zone is defined as a subsurface flow in which surface water and groundwater interact, mix and can return to the main channel.

Hyporheic exchange is an important component concerning transient storage due to variation in residence time, soil chemistry, microbial populations, anthropogenic effects, and aquifer properties compared to the main channel (Boulton et al., 1998, Runkel, 2002, Knust and Warwick, 2009). Transient storage lowers water velocity allowing for increased contact time of dissolved solutes and biogeochemically active sediments within the hyporheic zone (Runkel, 2002, Knust and Warwick, 2009). Biogeochemical refers to chemical changes driven by biological factors such as microorganisms within the subsurface such a nitrogen fixing bacteria, and geological factors such as sediment and minerals. Dissolved solutes undergo biogeochemical transformations, (Bencala et al., 1984, Constantz, 1998, Harvey and Fuller, 1998, Duff and Triska, 1990, Hill et al., 1998, Jones Jr et al., 1995, McMahon and Böhlke, 1996), within the subsurface, causing nutrients such as nitrogen, sulphur, and carbon to become more bioavailable. The presence of both oxidation and reduction reactions simultaneously taking place within the hyporheic zone are what make the hyporheic so biogeochemically active (Runkel et al., 2003).

2.3 Measuring Transient Storage

The transient storage model first described by Bencala (1983) has been used comprehensively in order to quantify both hydrodynamic and biogeochemical processes (Runkel, 2002) both of which are paramount for river restoration. Transient storage is typically measured using a conservative salt tracer of either Sodium Chloride or Sodium Bromide diluted with channel water. The tracer is injected into the channel and the time in which it travels across two known points downstream is recorded. A graph of time against concentration is plotted, known as a breakthrough curve or an advective/dispersive curve. This data is input into a transient storage model in order to quantify channel parameters and transient storage metrics. The simplest way of quantifying transient storage is using a 1D

(one dimensional) transient storage model. This method requires the solute mass to be uniformly distributed over the cross-sectional area of the channel, i.e. well mixed. However, this uniformity is rarely seen in nature, thus, only provides an assumption of channel parameters (Runkel and Chapra, 1993). In reality, the solute tracer is partially attenuated due to some tracer entering the transient storage zone (Runkel and Chapra, 1993). Therefore, two separate storage zones are considered. The first zone is the main channel and the second zone being the storage zone. The main channel zone processes influence solute concentrations, such as: transient storage, advection, dispersion and lateral inflow (Harvey et al., 1996). The storage zone includes areas such as recirculating pools, hyporheic zones and dead-end pore spaces (Bencala, 1983, Castro and Hornberger, 1991). These zones are connected mathematically using an exchange term that behaves as the mass transfer between both zones (Runkel and Chapra, 1993).

The first study to calculate a numerical relationship for the temporal movements of a transitional storage model was by Hays et al. (1966). This relationship was refined in a study done by (Nordin Jr and Troutman, 1980), which looked at a slug tracer released into a uniform channel. In this study, closed-form expressions (expressions that calculate a finite number of calculations) were published for the first-to-third temporal movements as derived from a Laplace transform of the transition storage equation put forward by Hays et al. (1966). Salt tracer injections coupled with 1D modeling allow for the interpretation of the transient storage zone's cross-sectional area and the transient storage exchange coefficient (Fernald et al., 2001). The most common modeling concept assumes a first-order mass exchange (this is an equation which links reaction rate with concentration), proportional to the difference in solute concentration between the main channel and the storage zone (Bencala, 1983, Bencala et al., 1990, Czernuszenko and Rowinski, 1997, Hays et al., 1966, Nordin Jr and Troutman, 1980). (1993) presented an implicit finite difference approximation for first-order mass exchange in the main channel and storage zone. This led to the development of the OTIS, which is one of the most used models in this field. OTIS stands for, One Dimensional Transport and Storage with Inflow and Storage model developed by Robert Runkel of the USGS in 1998 (Runkel, 1998). The OTIS model is a mathematical simulation, which describes the outcome of water-borne solutes in

both streams and rivers (Runkel, 1998). The model uses executable binary files that are configured to invoke the ANSI standard FORTRAN-77 compiler under the default optimisation, to calculate transient storage parameters from data located within the associated directories (Figure 1). The directories contain transient storage parameters, downstream conductivity measurements, and model parameters which can be manipulated using a text and source code editor in order to improve the model. The model and associated documentation is available for free on the USGS website (<https://water.usgs.gov/software/OTIS/>).

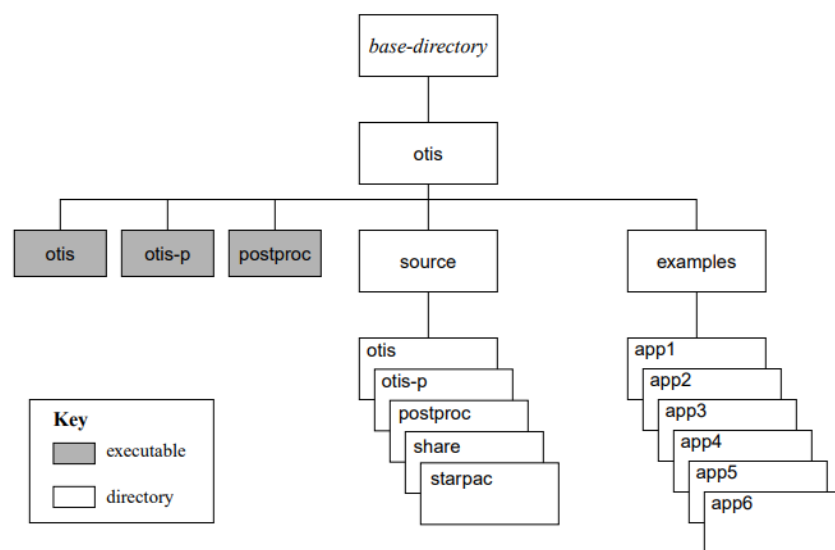


Figure 1: OTIS/OTIS-P Directory and Executable structure (Runkel, 1998)

2.4 Transient Storage Model Limitations

The use of advection-dispersion equations to give an output of the mean hyporheic residence times is related to the temporal length of the experiment, thus limiting transient storage calculation over a short time period. A similar issue was found by Gooseff et al. (2003), whereby the modified advection-dispersion equations assume that the residence time of water in storage within a channel is exponential, thus limiting any attempt to understand the solute arrival time of sub-stream locations via hyporheic flows. However, some studies have used residence time as a method of characterising hyporheic exchange (Haggerty et al., 2002, Wörman et al., 2002). These studies explain that this method is superior when compared to the advection-dispersion equations as the residence time distribution fits a simulated breakthrough curve similar to advection-dispersion but is not bound by the exponential residence time issue. It is clear in the literature that the storage zone is simplified to be considered a single large entity rather than

numerous smaller ones. However, a single large storage zone does not accurately describe transient storage (Becker et al., 2013, Choi et al., 2000). Limitations with the OTIS model must also be addressed; the most prolific issue with the OTIS model with regards to accurately modelling transient storage is that the interaction between channel flow and sub-channel flow is not clearly specified (Lin and Medina Jr, 2003).

2.5 Aims and Objectives

This study aims to quantify transient storage in both realigned and non-realigned reaches of the Swindale Beck in the Lake District, in order to determine the effectiveness and impact of river restoration from an ecosystem functioning perspective. The objectives of this study are as follows: (1) to quantify spatial patterns of transient storage both realigned and non-realigned reaches of the channel; (2) to quantify temporal patterns within realigned and non-realigned reaches from 2016 to 2017; (3) and to develop a conceptual model of transient storage to better understand the effects of river restoration and to aid in the development of future river restoration schemes.

3.0 Methods

3.1 Study Site

3.1.1 Swindale Beck Location and Catchment

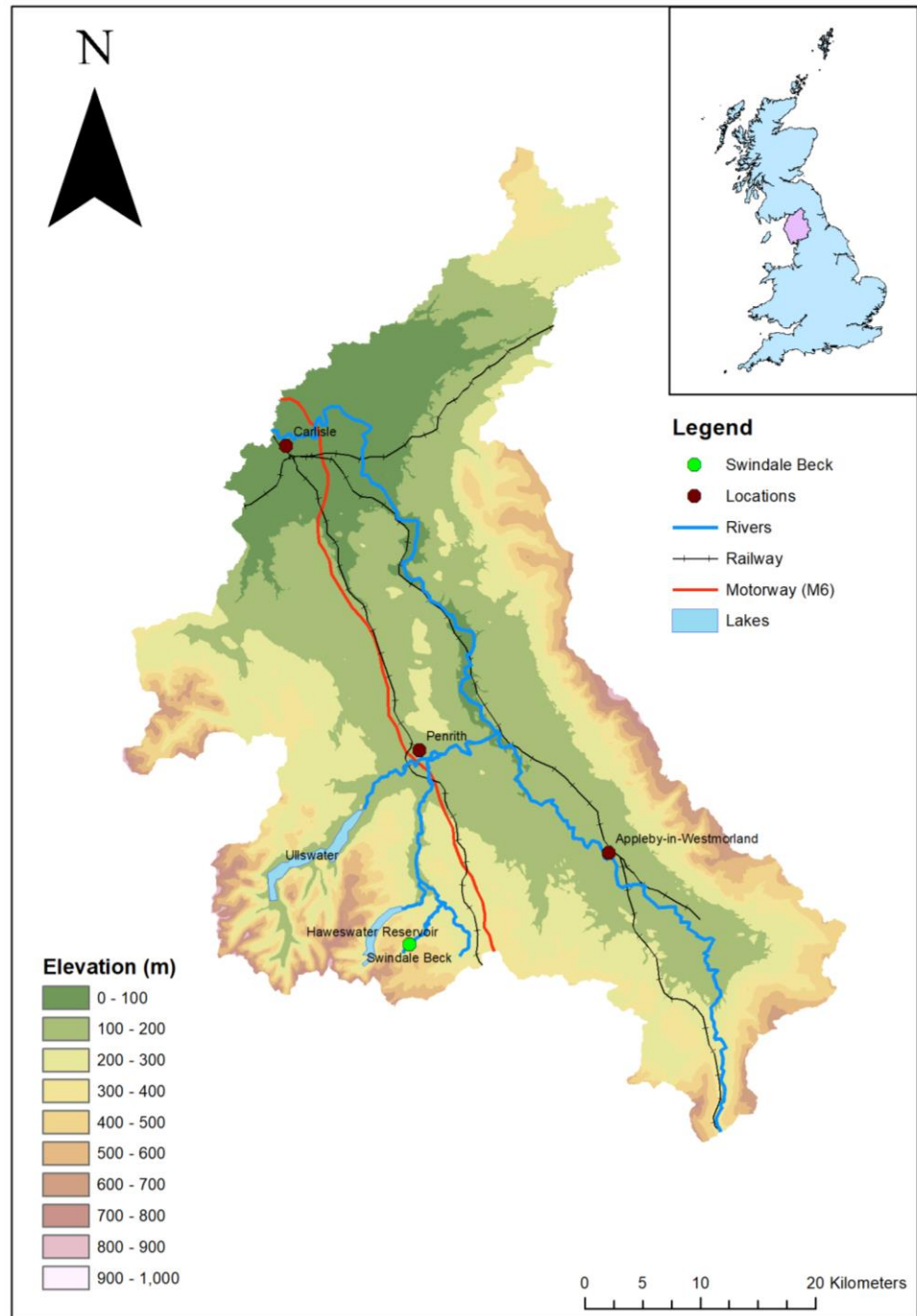


Figure 2: Swindale Beck topographical location within the Lake District. This map includes two towns and a city in order to provide context to the location of the Swindale Beck. Note the high elevation of Swindale Beck compared to the rest of the Lake District.

The river reaches used in this study were situated in the Swindale Beck in the Lake District, UK (Figure 2), and leased to the Swindale Farm. The catchment of the Swindale Beck consisted of a volcanoclastic sandstone and igneous andesite bedrock originating from the Borrowdale Volcanics. The bedrock was covered with

deposition diamicton, which were cultivated into agricultural grazing land. The river valley was a symmetrical V shape with the valley sides being elevated 100m higher than that of the valley floor with an angle of between 20 – 50 degrees. The valley floor was approximately 75 metres wide and composed of fluvial alluvium including: clay, sand, silt, and gravel.

It is well recognised that glaciers occupied the heads of many of the valleys within the Lake District during the Younger Dryas, and almost certainly impacted the formation and evolution of the valleys (Brown et al., 2011). The presence of moraines at the head of the valley, indicate that the catchment of the Swindale Beck underwent glacial processes. The glacial processes within the valley may be the source for much of the material deposited within the Swindale Beck (Church and Ryder, 1972). Evidence for this is that the Swindale Beck meanders through the moraines located at the head of the valley potentially transporting material from the moraines downstream. Before historical straightening, it is possible the channel eroded laterally across the floor of the valley allowing for the glacial sediment and debris to be entrained and deposited downstream (Church and Ryder, 1972), this could mean that glacial material eroded from the moraines is located across the valley floor.

The river was surrounded by a fragmentary riparian buffer strip, most of which was removed to increase the size of the cultivated grazing land, and levees which were constructed from channel materials by the landowner to prevent the river from meandering and overtopping during flood events. These measures aimed to preserve the grazing land and to prevent flooding. Alongside the grazing land was several SSSI hay meadows along the banks of the river. Meander scars were evident across the floodplain indicating the past natural river channel progression.

3.1.2 Swindale Beck Historical Straightening

Approximately 160 years ago, the Swindale Beck underwent straightening; first appearing in its straightened form in an 1869 OS map. The landowner reinforced the riverbanks with material taken from the channel and created levees to prevent overtopping during flood events in order to protect the farmland. Levee construction and bank reinforcement subsequently led to an increase in downstream velocity. This, coupled with a lack of channel meandering, led to the

formation of a channel with uniform width and depth, and an absence of naturally forming riffles, pools, and sandbars. The levees and reinforced banks acted to cut off the channel from the surrounding floodplain, denying the transfer of nutrients and organic matter from the floodplain (Tockner and Stanford, 2002, Baker and Vervier, 2004). During flood events the overtopping of the levees led to floodwater being unable to return to the channel instead pooling on the surrounding land, becoming stagnant, reducing the agricultural value.

3.1.3 Restoration Efforts

Restoration of the upper Swindale Beck began in 2016, with the aim of re-meandering a section of the river, and the removal of the reinforced banks and levees (Figure 3 and Figure 4). Using a detailed topological map, alongside the evidence of paleo-channels before the channel was straightened, the Environment Agency (EA) designed a more suitable channel. This route, however, went through a SSSI hay meadow, which resulted in the heavy machinery only being permitted to operate within the footprint of the river in order to mitigate the disturbance to the SSSI site. Work began on March 2016, replacing 750 metres of the old channel with 890 metres of the realigned meandering channel. In addition, 110 metres of channel was created in order to reconnect existing tributaries to the realigned channel. The former channel was back filled with the spoil from the realigned channel and reseeded with brush from the SSSI site. The bridge which was used to provide access to the south side of the channel was removed and was replaced with a ford. This was undertaken in order to prevent restrictions to natural channel progression and meandering. In 2017, 436 metres of upstream river channel underwent the creation of riffle forming structures in the main channel. This method is less invasive than digging an entirely new channel, yet still accelerates channel morphological change. This river restoration scheme is part of a large catchment management plan designed to alleviate flooding and to promote ecosystem rehabilitation. These methods would imply that the Swindale Beck restoration is primary process-based but uses form-based techniques in order to potentially accelerate the restoration process. This technique has been used in other restoration schemes to achieve the same effect (Wohl et al., 2015).

River steering structures were constructed in two locations, between SB2DS and INJ1, and at SB3US (Figure 4). The river steering structure at SB3US was made up

of boulders removed from the paleo-channels during the river restoration and placed along the south riverbank in order to prevent the realigned channel from returning to the old channel. The introduction of a steering structure in-between SB2DS and INJ1 was in order to prevent the realigned reaches from returning to the mature straightened channel. This was composed of wooden railway sleepers and boulders taken from the realigned channel. Located on the opposite bank were the remains of the old channel which have not been infilled as of 2018. This led to the formation of a large pool within the non-realigned channel and meant that a study reach could not be located here, as it would have a negative impact on the modelling method used in this study. Sapling trees were planted along either side of the banks along the SB2 reach during the restoration efforts. This was in order to stabilise the banks and to assist draining in this area as surface water storage zones were evident along the reach and upon the floodplain. A river inflow point was located along the northern bank just upstream of the SB2 Injection Point. (In Figure 4 it seems like the injection site was upstream of the lateral inflow point but in reality, the injection took place downstream for the inflow point).

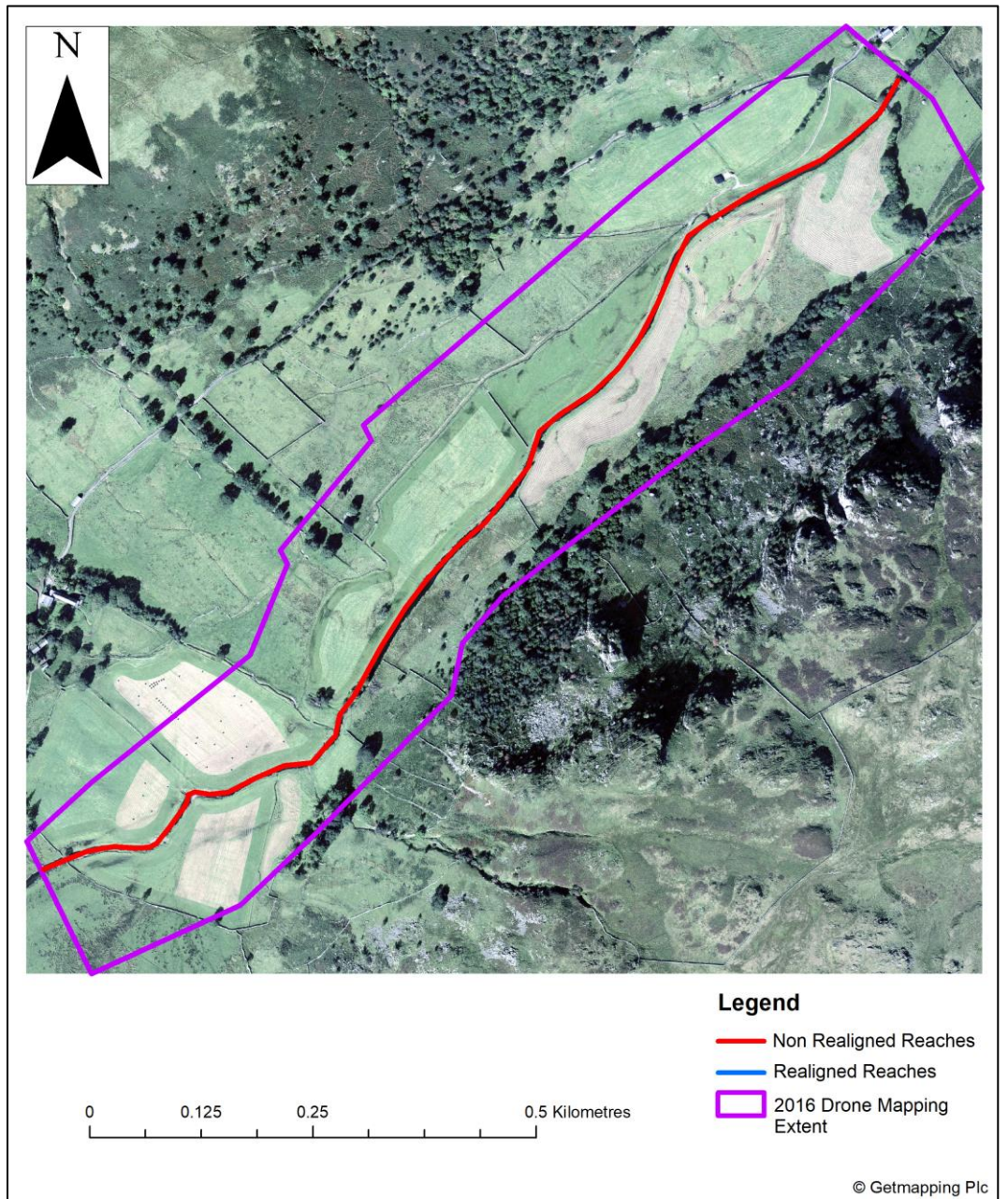


Figure 3: Swindale Beck reach extent during 2015 prior to restoration. Note, no restoration efforts had taken place in 2015, and thus the reaches had not been delineated.

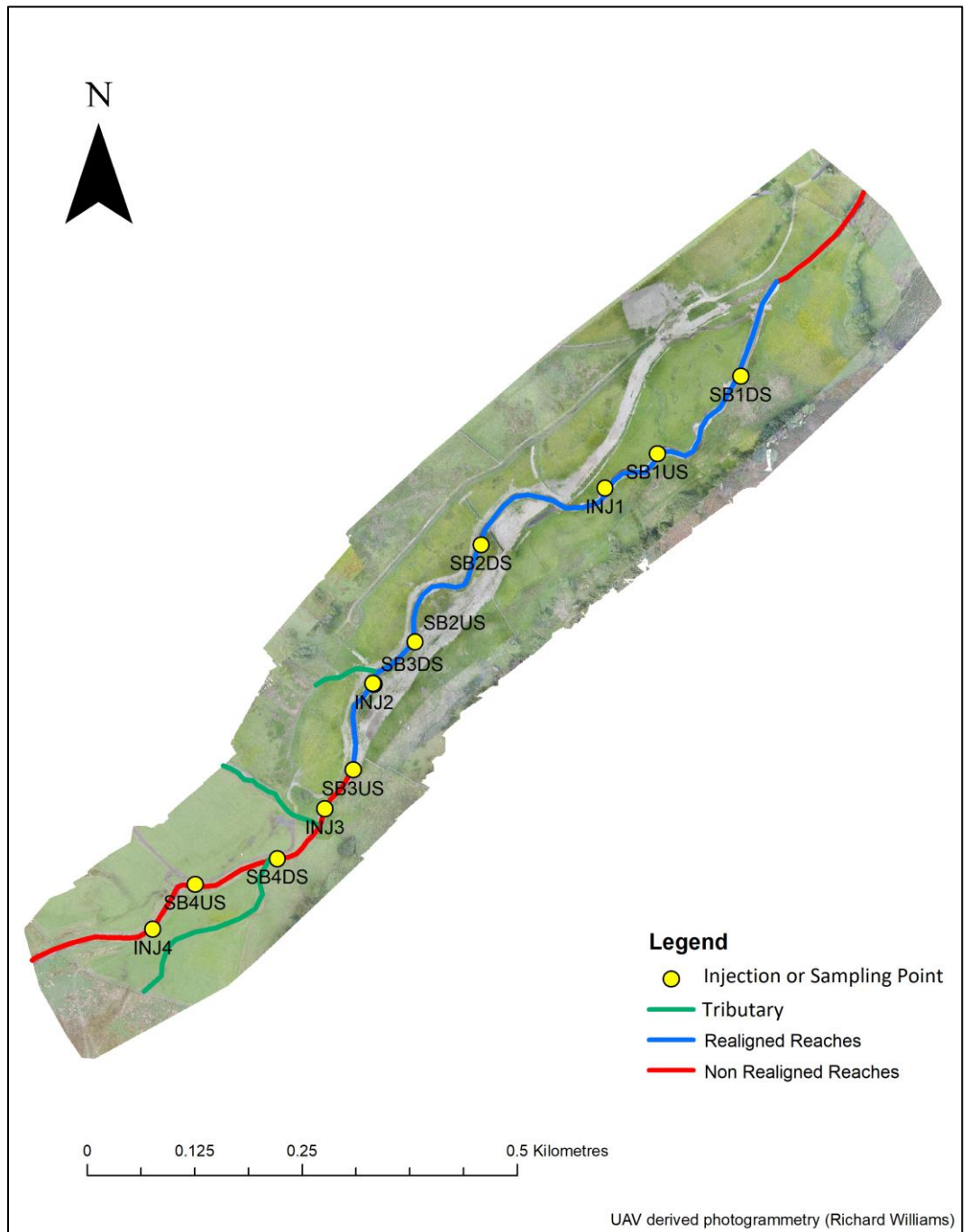


Figure 4: The location of the realigned and non-realigned reaches. Note, INJ2 and SB3DS are the same points.

The blue and red lines in Figure 3 and Figure 4 indicate the extent of restoration efforts for each year. For this reason, Figure 3 has no blue line during 2015 as no restoration work had been undertaken. The proximity of SB2 reach and SB3 reach is evident in Figure 5. This was due to a deep pool, located after the SB2 reach, which would have attenuated the tracer, leading to an increase travel times which would not be appropriate for monitoring. Thus, the reach had to be located upstream of the pool whilst maintaining sufficient reach length to allow for adequate mixing within the channel.

3.2 Tracer Injection Methodology

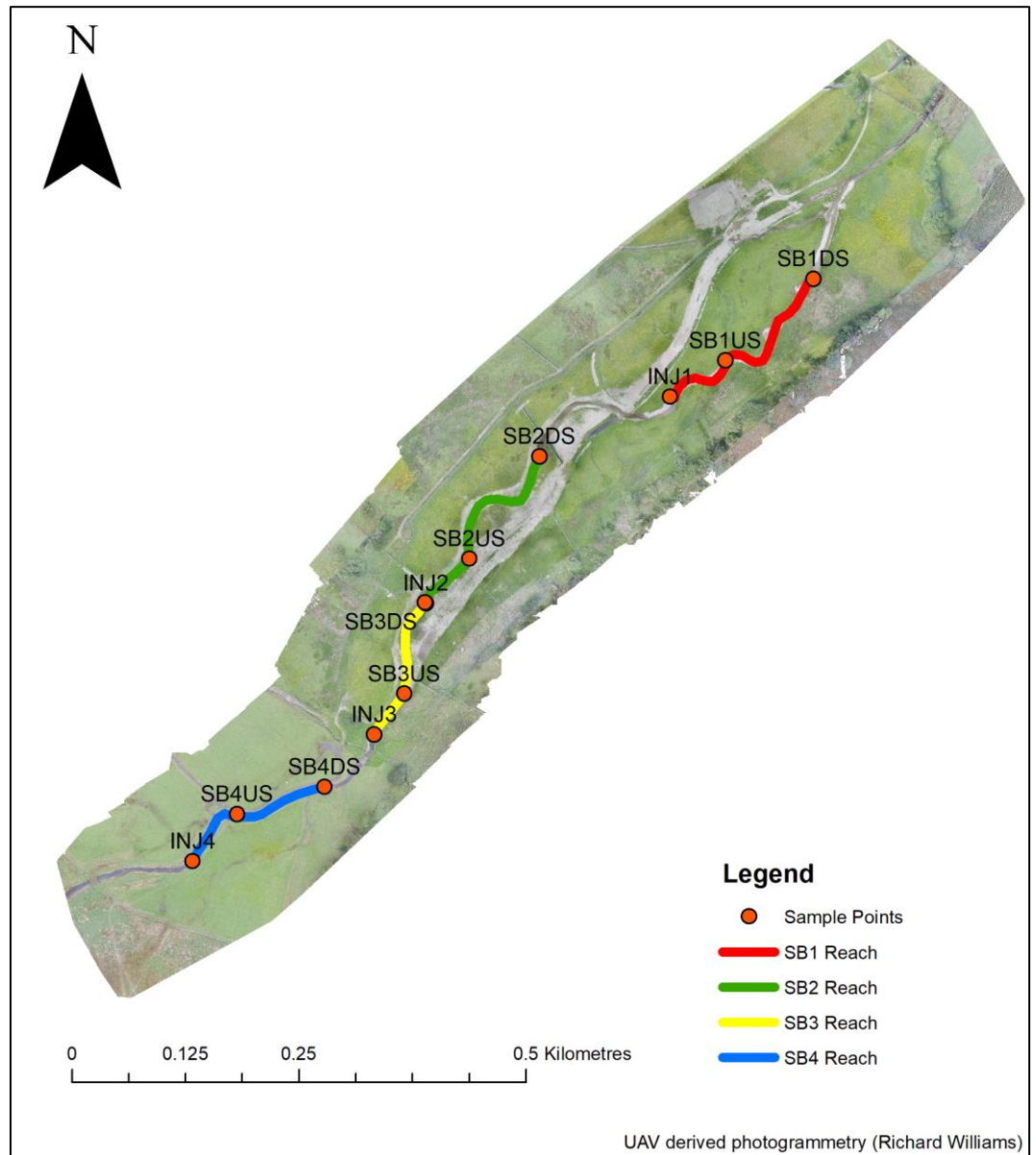


Figure 5: Swindale Beck delineated into the SB4, SB3, SB2 and SB1 reach.

Four study reaches were delineated to represent three realigned reaches and one non-realigned reach (Figure 5). The realigned reaches were labelled: SB1, SB2, and SB3 whilst the non-realigned reach was labelled SB4. SB3 was identified as realigned because the majority of the reach underwent restoration. A small upstream section was left non-realigned as this section consisted of small natural cascades and rapids formed around very large boulders that would have difficult to remove and the rapids provided a unique habitat that was not present in other reaches. As this reach was partially realigned it cannot be classified as completely non-realigned. Based on the stream reconnaissance handbook (Thorne, 1998), and using the Wentworth grain size classification (Wentworth, 1922) a

representative reach survey was conducted on the 16th of September 2016, and the 27th of September 2017, to establish reaches appropriate for the scientific method. For this experiment, it was decided to use a solute tracer injection to measure discharge as described by (Kilpatrick and Cobb, 1985). For each of the established reaches, a conservative tracer was created by thoroughly mixing 5Kg of NaCl during 2016 and 12.5kg of NaCl during 2017, with 50L of river water to achieve a tracer concentration of 100g/L NaCl in 2016 and 250g/L NaCl in 2017. The increased mass of NaCl used in 2017 is due to the ideal conductivity of the tracer being at approximately 200% above background (Moore, 2005). The NaCl tracer was introduced into each reach via a slug injection which was performed upstream of the reach that was under investigation. This study used two PCE-PHD-1 multifunction pH meters that logged the change in electrical conductivity (breakthrough curve) at five-second intervals from the centre of the channel, approximately 20m downstream from the injection site. These two sites were labelled upstream (US) and downstream (DS) (Figure 5). During the five seconds between each reading, the NaCl value could change rapidly, causing the initial rise to appear much steeper than it was in reality. In order to lessen this the mean average of each value and the subsequent value was calculated for the entire dataset. The discharge of both the upstream and downstream of each reach was calculated by dividing the mass of NaCl used in the tracer by the area under the breakthrough curve ($Q = M/A$).

Where,

Q	-Discharge [m^3/s]
M	-Mass of salt tracer [mg]
A	-Area under the breakthrough curve [hr*mg/L]

3.3 Modelling Methodology

3.3.1 Transient Storage Modelling

The OTIS and OTIS-P models use solute tracer concentration values in order to estimate transient storage parameters rather than electrical conductivity values. In this study, as electrical conductivity was measured instead of NaCl concentration, a calibration between the NaCl and electrical conductivity was determined.

This allowed for the electrical conductivity values to be converted into NaCl concentrations for use in the OTIS and OTIS-P models. The OTIS and OTIS-P models can only function with less than 200 data points, which was substantially less than the number logged in this study. In order to accommodate this limitation data was systematically removed in order to reduce the number of values without impacting the trend of the data. The upstream dataset was input into the OTIS model. The model would then attempt to simulate the downstream data set using the transient storage parameters approximated for the reach. These parameters were adjusted manually until the downstream data set predicted by the OTIS model correlated with our observed downstream data (see Appendix). These updated transient storage parameters were input into the OTIS-P model (a modified version of the OTIS model), which results in improved transient storage parameters estimated using a non-linear regression function. The improved transient storage parameters were input manually back into the OTIS-P model for each subsequent run. This method was continued until the estimated transient storage parameters no longer changed, meaning that the OTIS-P model had determined the river reach parameters according to our measurements. These parameters were used to calculate the seven transient storage metrics used in this study.

3.3.2 OTIS Model Parameters

The OTIS model uses a pair of differential equations to estimate transient storage parameters.

$$A) \frac{\partial C}{\partial t} = -\frac{Q}{A} * \frac{\partial C}{\partial x} + \frac{1}{A} * \frac{\partial}{\partial x} \left(AD * \frac{\partial C}{\partial x} \right) + \frac{Q_{lin}}{A} * (C_{lin} - C) + \alpha(C_{stor} - C)$$

$$B) \frac{\partial * C_{stor}}{\partial t} = \alpha \frac{A}{A_2} * (C - C_{stor})$$

Where,

C	-main channel solute concentration [gm ⁻³]
t	-time [s]
Q	-volumetric flow rate [m ² s ⁻¹]
A	-main channel cross-sectional area [m ²]
X	-distance [m]
D	-dispersion coefficient [m ² s ⁻¹]
Q _{lin}	-lateral inflow rate [m ³ s ⁻¹ m ⁻¹]

C_{lin}	-lateral inflow solute concentration [gm^{-3}]
α	-storage zone exchange coefficient [s^{-1}]
C_{stor}	-storage zone solute concentration [gm^{-3}]
A_2	-storage zone cross-sectional area [m^2]

Equation B is an inverse solution to equation A, using a Crank-Nicolson finite-difference solution to approximate spatial derivatives. The percentage difference between the upstream and downstream breakthrough curves give an indication as to whether there is a net increase or decrease of water within the river between the upstream and downstream zones.

3.3.3 OTIS Transient Storage Parameter Estimates

Initial data for the OTIS model consisted of data collected from the upstream monitoring location. This included: the calculated discharge (Q), main channel cross-sectional area (A), dispersion coefficient (D). Discharge estimates were made using calculations of data from the saline tracer injection. Main channel cross-sectional area estimates were derived by first calculating the travel time of the tracer from the electrical conductivity measurements (this was the time difference between the midpoint of the rise of both upstream and downstream saline tracer graphs see Figure 6.) Storage zone exchange coefficient (α) and storage zone cross-sectional area (A_2) was not needed for the first OTIS run as the first run only models advection and dispersion. Thus, α was set to zero and A_2 was set to an arbitrary value (this value must be set to a value that is not '0', if zero is used the model will attempt to divide by zero and fail, however, any other value will not affect the model unless the mechanism is enabled). The reach length divided by the travel time gave the average velocity of the channel water within the reach. The velocity divided by the discharge gives the main channel cross-sectional area.

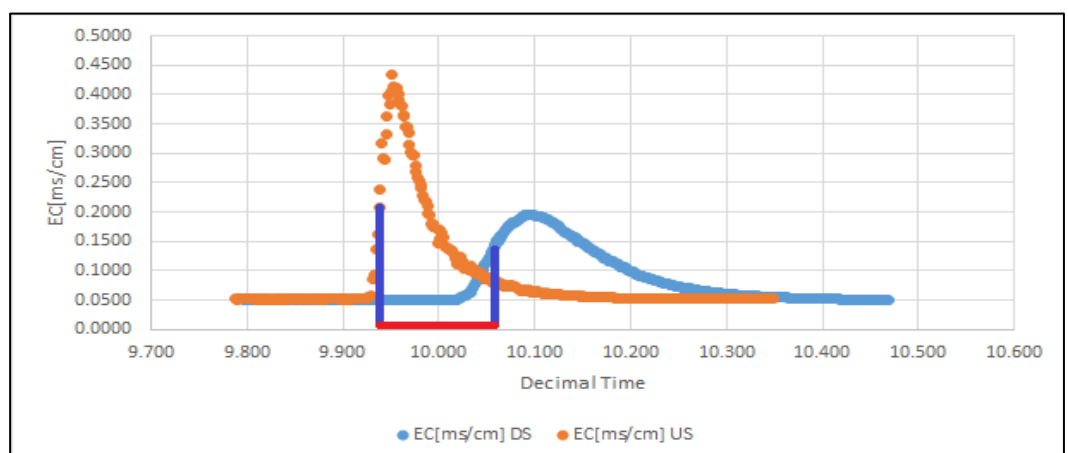


Figure 6: The red line shows the time period which was used to calculate cross-sectional area of the channel.

The dispersion coefficient was unknown for the first OTIS run and a value of one was used in order to provide a starting point. The lateral inflow rate Q_{lin} was left as zero due to the lack of inflow indicators within each reach and was not measured in the field. This also simplified the model substantially, allowing for much faster processing times.

3.3.4 Transport Simulations

Using the parameter estimates outlined above and the observed upstream breakthrough data, the downstream breakthrough curve was estimated. The observed and simulated downstream breakthrough curves are then matched using manual adjustment of the parameters. Increasing and decreasing the 'A' and 'D' values allowed for the best fit to be obtained of the simulated and observed downstream breakthrough curves to be obtained (Appendix). When the simulated downstream breakthrough data matched the simulated data, the hydrodynamic parameters were used as initial estimates for OTIS-P. OTIS-P determines a set of optimised parameter estimates that minimise the squared differences between the simulated and the observed breakthrough curves. This process effectively automates the parameter estimation procedure. This allows for more precise alteration to be made to the hydrodynamic parameters more rapidly than if it were done manually.

OTIS-P was run in two stages. The first stage involved running the OTIS-P model without α and A_2 enabled, in order to increase the accuracy of the A and D values. The model was more complex, and failure was more likely when α and A_2 values were enabled as the model was more likely to find false convergence. In turn running OTIS-P before enabling α and A_2 helps to negate this. The OTIS-P model provides estimates of likely values for each enabled transient storage parameter. These new values replace the previous transient storage parameters and model is re-run. This process was continued until the transient storage parameter estimates did not change any further, which identified the calculated transient storage parameters for the reach. The accuracy of the parameters was verified, as the simulated downstream breakthrough curve should match exactly on to the observed downstream breakthrough curve if the parameters correct. The final parameters were then used in the calculation of the transient storage metrics.

Tests for normality were conducted on the transient storage parameter estimates and transient storage metrics using the SPSS software platform in order to determine the appropriate statistical test and to determine significant differences (Appendix Table 8, and Table 10, respectively). Due to both the transient storage parameter estimates and transient storage metrics having a low number of values, the Shapiro-Wilk normality output was selected. The normality test for the transient storage parameter estimates found the data to be normal, thus, the non-parametric Mann-Whitney U test was selected to test for statistical significance. Concerning the transient storage metrics, two of the transient storage metrics were found to be non-normal whereas the remaining transient storage metrics were normal. SPSS recommends that in this situation to use a non-parametric test, thus a Mann-Whitney U test was selected.

3.3.5 Transient Storage Metrics

A total of seven different metrics for transient storage were used for each year of study (2016 and 2017) and are described below.

1) Damköhler number (Dal)

Wagner and Harvey (1997) developed a method for determining the reliability of parameter estimates for tracer modelling studies. This method used the dimensionless number called the Damköhler number (Dal) as an indicator of the parameter identifiability. The Damköhler number is a ratio of the storage exchange rate and the main channel advection rate where the optimal range of values is between 0.1 and 10.0 (Harvey and Wagner, 2000).

$$Dal = \frac{\alpha \left(1 + \frac{A}{A_2}\right) L}{u}$$

Where,

α	-storage zone exchange coefficient [s^{-1}]
A	-main channel cross-sectional area [m^2]
A_2	-storage zone cross-sectional area [m^2]
L	-reach length [m]
u	-average stream velocity [ms^{-1}]

2) $F \frac{200}{Med}$ (FMed@200)

FMed@200 [%] is the percentage of median transport time due to transient storage, this provides a normalized metric allowing for the comparison of transient storage between different length reaches, as the length for each reach is calculated as if they are 200m long.

$$F \frac{200}{Med} = (1 - e^{-L\frac{\alpha}{u}}) \frac{A_2}{A + A_2}$$

Where,

L	-200 metres [m]
α	-storage zone exchange coefficient [s^{-1}]
u	-stream velocity [ms^{-1}]
A_2	-storage zone cross-sectional area [m^2]
A	-main channel cross-sectional area [m^2]

3) Residence time in the transient storage zone (TimeStor)

Residence time in the transient storage zone [seconds] is the amount of time a parcel of stream water spends within the storage zone and was first described by Thackston and Schnelle (1970).

$$Timestor = \frac{A_2}{\alpha * A}$$

Where,

α	-storage zone exchange coefficient [s^{-1}]
A_2	-storage zone cross-sectional area [m^2]
A	-main channel cross-sectional area [m^2]

4) Storage zone turnover length (Ls)

Storage zone turnover length [metres] is the average length that a stream water parcel travels before being exchanged with storage zone. This was first described by Harvey et al. (1996).

$$Ls = \frac{u}{\alpha}$$

Where,

u	- stream velocity [ms^{-1}]
α	-storage zone exchange coefficient [s^{-1}]

5) Standardised storage zone area (TranStor)

Standardised storage zone area [%] is the percentage of the main channel which is the storage zone.

$$TranStor = (A_2/A)*100$$

Where,

A_2 -storage zone cross-sectional area [m²]
 A -main channel cross-sectional area [m²]

6) Storage zone exchange flux (qs)

Storage zone exchange flux [m³/s/m], describes the water flow rate per unit area, i.e. the amount of water that flows through a cross-section of the storage zone per second, and was described by Harvey and Wagner (2000), Harvey et al. (1996).

$$qs = \alpha * A$$

Where,

α -storage zone exchange coefficient [s⁻¹]
 A -main channel cross-sectional area [m²]

7) Hydrologic retention factor (Rh)

Hydrologic retention factor [s/m]. This metric quantifies storage zone resistance time of stream/river water per unit of stream reach travelled, and first described by Morrice et al. (1997). In effect, this means the storage zone residence time per metre of stream reach travelled by surface water before entering the subsurface storage zone. This is accomplished by considering the relationship between stream transport and the hydrodynamics of the storage zone, thus allowing for comparisons of hydrological retentions to be made between separate river systems.

$$Rh = \frac{TimeStor}{Ls}$$

Where,

Timestor -residence time in the transient storage zone [s]
Ls -storage zone turnover length [m]

3.4 Geomorphic Unit Analysis

Aerial photography captured the site of the restoration project during 2016 and 2017. This was undertaken using a DJI Phantom 4 Professional UAV equipped with a 1-inch 20-megapixel complementary metal-oxide-semiconductor image sensor (DJI, 2019) to capture images of the study site at an altitude of 50m. Geomorphic unit analysis was conducted in order to observe the changes in river morphology in the realigned reaches from 2016 to 2017. This analysis was not possible in the non-realigned reach as the UAV derived photogrammetry did not encompass the SB4 reach during data collection in 2017. Cross-sections of each reach (Figure 12) and a long profile all four reaches were digitised (Figure 11). For the long profile data collected during 2017 was used for the realigned reaches data collected whereas in the non-realigned reaches data collected during 2016 was used. This was followed by statistical analysis of geomorphic units (riffles, pools, and sandbars), to determine statistical significance using the SPSS software platform. The data was verified through a river reach survey (Appendix Table 18), which allowed for finer details of the channel to be collected that were not revealed by the aerial photography due to resolution limitations, such as: bank characteristics bank materials, average bank slope and torsion cracks, bank face vegetation, and bank erosion.

The sampling approach used in the river reach survey involved the use of Section C of the stream reconnaissance handbook (Thorne, 1998), and used the Wentworth grain size classification (Wentworth, 1922). This section of the reconnaissance handbook focuses on the river from and was undertaken in order to proof the UAV derived photogrammetry. In this study the left and right bank are the true left and true right banks. Sampling was conducted within each reach and the information described in the river reach survey describes the average characteristics within the reach (Appendix Table 18).

Aerial photography was analysed using the ESRI ArcGIS software package in order to digitise and quantify geomorphic units alongside creating channel cross sections

and a long profile of the four study reaches. River cross-sections were calculated using the cross-section tool in ArcGIS. Cross-sections were drawn approximately 25 – 30m long, crossing the river at 90 degrees at the four injection points, four upstream monitoring points and four downstream monitoring points (Figure 7). The long profile of the Swindale Beck was calculated using the cross-section tool in ArcGIS, instead of using this tool in the conventional fashion, a single “cross-section” was taken along the length of the river (Figure 11). The riffles, pools, and sandbars were digitised manually in ArcGIS and the total area for each geomorphic unit was determined for the years 2016 and 2017 including the total area of all geomorphic units combined. This data was analysed in SPSS in order to determine whether there was any statistical significance between the 2016 data and the 2017 data. Tests for normality were conducted to select an appropriate parametric/non-parametric test to test for significant differences for the area of sandbars, pools, and riffles (Appendix, Table 12, Table 13, Table 14, respectively). Due to the low number of values, the Shapiro-Wilk output was selected. For the sandbars data (Bars), a T-Test was selected as the data was determined to be normal, (Appendix Table 15). The pools data (pools) was determined to be non-normal and thus a Mann-Whitney U test was selected (Appendix Table 16). The data for the riffles (riffles) was determined to be normal for the 2016 data but non-normal for the 2017 data. In this situation SPSS recommends to use a non-parametric test, so a Mann-Whitney U test was selected, (Appendix Table 17). The 2017 data for riffles, pools, and sandbars in realigned reaches were compared to the 2016 data, and the percentage change was calculated between the two years (Table 7).

4.0 Results

4.1 OTIS Model Parameters

Figure 7 illustrates the similarity between the observed breakthrough curves collected on site and the simulated data that was predicted by the OTIS-P model. This demonstrates the accuracy of the parameters used in the OTIS-P model. It is important to note that the SB4 2016 and SB2 2017 graphs (Figure 7) shows the furthest deviations from the observed data. This may be explained by low level lateral inflows that were not easily visible during reach delineation (Figure 7). The closer the fit between the observed data and the simulated data the more

confident we can be that the channel parameters describe the channel accurately. Table 1 and Table 2 indicate the area under upstream (US) and downstream (DS) breakthrough curves that were taken in the field. The positive and negative percentage changes indicates lateral inflow and outflow respectively. The relatively low levels of lateral inflow and outflow observed permit the omission of lateral inflow modelling within the OTIS-P Model. Lateral inflow modelling increases the complexity of the model and is not ideal.

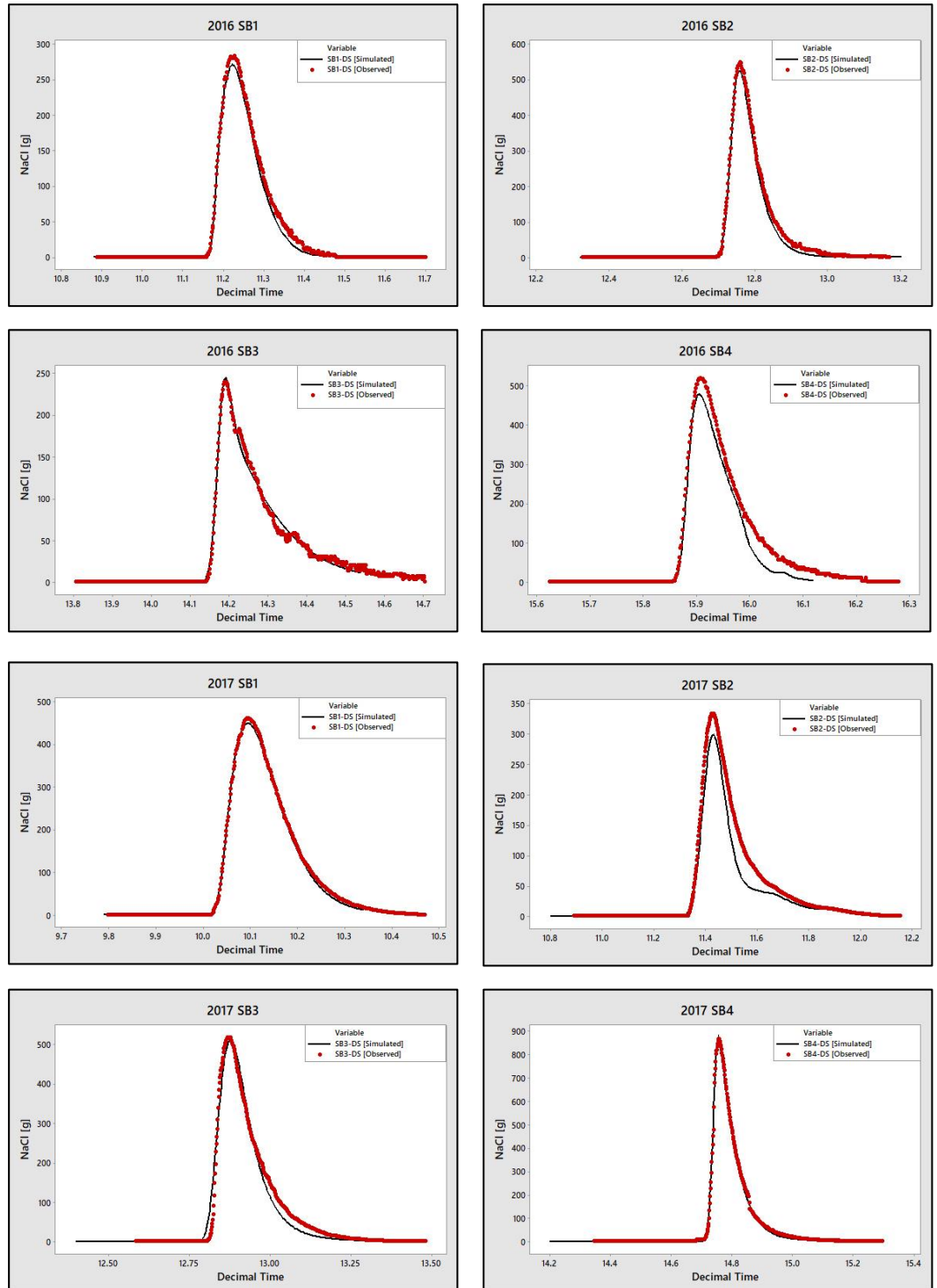


Figure 7: Illustrates the difference between the data collected in the field (Observed) and the data simulated by the OTIS model (Simulated). 2016 SB1 and SB2 along with 2017 SB1, and SB4 show the best fit between the observed and simulated data. 2016 SB3, and 2017 SB3 have a good fit but it is not as close as the aforementioned reaches. 2016 SB4 and 2017 SB2 have the weakest fit between observed and simulated data.

The difference between the upstream and downstream reaches is evident in Table 1 and Table 2. When the conductivity results from the salt injection were illustrated graphically, the upstream breakthrough curve will have a steep rising and falling limb with a high peak concentration. Compared to the downstream reach, which will have a shallower rising and falling limb, with a lower peak

concentration (Figure 6). If the percentage change between the area under each of the breakthrough curves is low then the majority of the tracer has passed from the upstream reach to the downstream reach implying low levels of lateral inflow.

Restored Reaches			
Reach	US area under BTC	DS area under BTC	Percentage Change
SB1 2016	2.86	3.13	8.59%
SB1 2017	6.63	6.23	-6.43%
SB2 2016	4.51	5.05	10.82%
SB2 2017	4.90	5.74	14.71%
SB3 2016	3.36	3.30	-1.89%
SB3 2017	7.44	7.14	-4.26%

Table 1: Area under the breakthrough curves (BTC) for the realigned reaches for 2016 and 2017

Reach	US area under BTC	DS area under BTC	Percentage Change
SB4 2016	4.75	5.37	11.59%
SB4 2017	8.05	7.56	-6.47%

Table 2: Area under the breakthrough curves (BTC) for the non-realigned reaches for 2016 to 2017

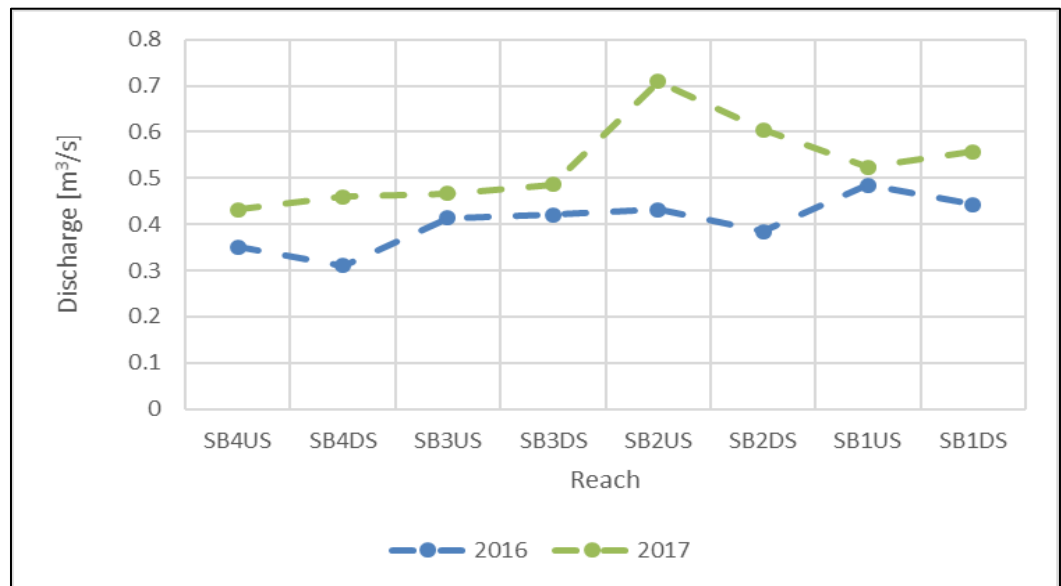


Figure 8: Calculated discharge for the upstream and downstream of each reach during 2016 and 2017. It is important to note that the graphs starts at SB4 and moves downstream to SB1, this is to allow easier comparison to other figures.

The calculated discharge was found to be higher in all reaches during 2017 compared to 2016 (Figure 8). This was due to increased rainfall prior to data collection during 2017. The discharge for SB2US during 2017 is 64% higher than in 2016. This large variation in discharge could be due to lateral inflow within the reach (Table 1 and Table 2). However, the other reaches had dispersion values that were very similar from 2016 to 2017.

The variation in calculated OTIS parameters for the realigned and non-realigned reaches is displayed as box and whisker plots (Figure 9). It is important to highlight that these plots do not illustrate the variation in data appropriately from 2016 to

2017 due to the limited number of values. Dispersion values (D) were 150 higher in non-realigned reaches than that of the realigned reaches (Table 3 and Table 4). The values for D during 2017 were higher than the values for 2016 in all reaches except SB2, this was most likely due to SB2 being a less than ideal reach during 2017 due to the presence of deep pools after the injection point and potentially with low levels of lateral inflow. These deep pools can attenuate tracer leading to inaccurate discharge values. Main channel storage area (A) values were 77% higher in realigned reaches than that of non-realigned reaches. SB2 shows the largest change between 2016 to 2017, this, like with D, is probably due to deep pools forming within the reach between 2016 to 2017. Storage Zone Area (A²) values were 79% higher in realigned reaches than that of non-realigned reaches. SB3 2016 shows the highest value, being nearly double the second highest value. Storage zone exchange coefficient (α) values were on average very similar in realigned reaches and non-realigned reaches. All reaches except SB1 experienced an increase in α from 2016 to 2017. Velocity (V) values were 30% higher in non-realigned reaches than that of realigned reaches. Despite having the highest gradient (Figure 11), SB3 had the lowest calculated water velocity (Table 3 and Table 4). Similarly, despite SB2 having the lowest gradient (Figure 11) the calculated velocity was greater than that of SB3, which has a greatest gradient (Table 3 and Table 4). This may be caused by the increased hydraulic head experienced in the realigned reaches compared to that of the non-realigned reaches.

Restored Reaches						
Reach	D [m ² s ⁻¹]	A [m ²]	A ² [m ²]	α [s ⁻¹]	V [ms ⁻¹]	Q m ³ /s
SB1 2016	0.002	1.393	0.473	0.007	0.348	0.485
SB1 2017	0.293	1.249	0.566	0.006	0.419	0.524
SB2 2016	0.085	1.616	0.255	0.003	0.267	0.431
SB2 2017	0.002	2.316	0.600	0.005	0.306	0.709
SB3 2016	0.051	2.392	1.052	0.002	0.173	0.414
SB3 2017	0.189	1.661	0.651	0.004	0.281	0.466
Means	0.104	1.771	0.599	0.004	0.299	0.505

Table 3: Parameters for the realigned reaches calculated by OTIS-P for 2016 and 2017. D = Longitudinal Dispersion, A = Main Channel Area, A² = Storage Zone Area, α = Exchange Parameter, V = Velocity. The mean values aid in identifying values which a greater than average.

Unrestored Reaches						
Reach	D [m ² s ⁻¹]	A [m ²]	A ² [m ²]	α [s ⁻¹]	V [ms ⁻¹]	Q m ³ /s
SB4 2016	0.122	0.960	0.245	0.003	0.366	0.351
SB4 2017	0.400	1.038	0.422	0.005	0.416	0.431
Means	0.261	0.999	0.334	0.004	0.391	0.391

Table 4: Parameters for the non-realigned reaches calculated by OTIS-P for 2016 and 2017.

Parametric tests found no significant difference between calculated OTIS parameters for 2016 or 2017 (Appendix, Table 9). Figure 9 illustrates the difference in calculated parameters between the realigned and non-realigned reaches in the form of box and whisker plots. It is clear in Figure 9 that for each parameter, the non-realigned reaches show less range than that of the realigned reaches, this would imply less variation in the channel. However, it is clear there are significantly less values for the non-realigned reaches which may also be influencing this trend. Mean values for dispersion and velocity are higher in non-realigned reaches compared to realigned reaches; whereas main channel area, storage zone area, and the exchange parameter all show greater mean values for the realigned reaches. Only the exchange parameter shows a positive skewness in the realigned reaches, whereas the other parameters all have negative skews. The skewness of the box and whisker plots (Figure 9) also confirms the lack of normality that was found by the parametric tests.

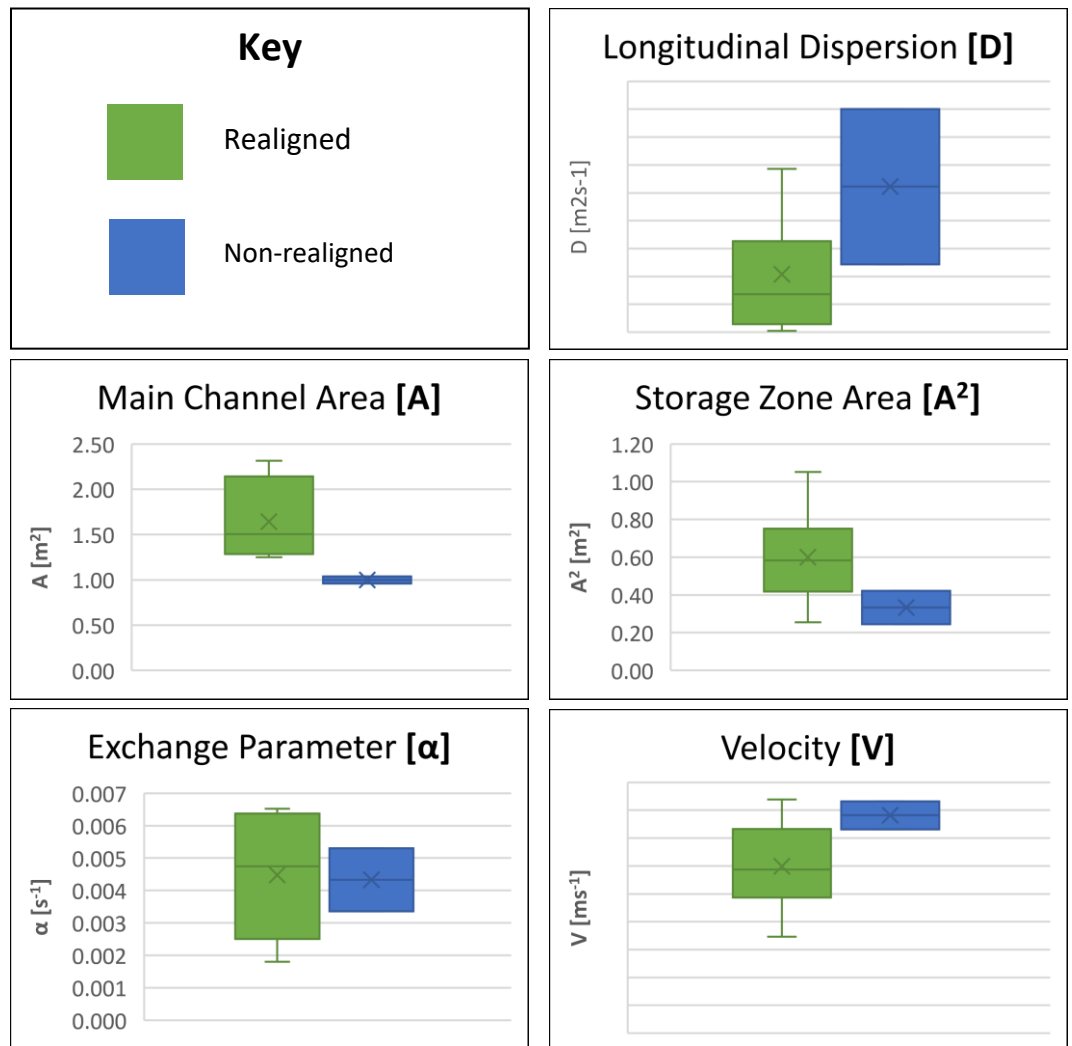


Figure 9: Box and Whisker Plots describing the data displayed in Table 3 and Table 4.

4.2 Transient Storage Metrics

The Mann-Whitney U test found there was no significant difference between 2016 and 2017 transient storage metrics (Appendix, Table 11). The Damköhler (Da) values calculated for the four reaches for both 2016 and 2017 indicate that adequate mixing took place in the reaches SB1 during 2017, SB3 and SB4 for both 2016 and 2017. However, the reaches SB1 2016 and SB2 2016 and 2017 did not experience adequate mixing as the Da value was greater than 10 (Table 5). There is the possibility that SB1 2016 was less affected by the inadequate mixing than SB2 2016 and 2017, due to the similarity with SB3 and SB4 metrics (Table 5 and Table 6), whereas SB2 has a much greater variation in metrics.

FMed@200 indicates that within realigned reaches, transient storage made up on average 23.3% of travel time, with a range of 11.9% - 29.6% (Table 5), whereas, transient storage in non-realigned reaches made up on average 21.9% of travel time with a range 17.1% - 26.8% (Table 5). It is clear that the realigned reaches

have a greater average FMed@200 value than the non-realigned reaches alongside a larger range of values (Table 5 and Table 6).

Residence time in storage (TimeStor) was found to be on average 64.4 seconds within realigned reaches with a range of 50.1 – 90.8 seconds (Table 5). In the non-realigned reach the average value was found to be 76.3 seconds, and a range of 75.8 - 76.7 seconds (Table 6). Table 5 shows the value for SB3 2016 to be crossed out. This was because this value was determined to be an outlier and subsequently was removed from the mean calculation.

Storage zone turnover length (Ls) was found to be on average 72.8 metres within realigned reaches with a range of 53.4 – 97.4 metres (Table 5). Whereas non-realigned reaches experience a much larger average value of 93.6m and a range of 78.4 – 108.7 metres (Table 6). The non-realigned reach SB4 2016 has the highest storage zone turnover length of 108.7 metres (Table 6), whereas the realigned reach SB1 2016 has the shortest with 53.4m (Table 5).

Standardised storage zone area (TranStor) was found to be on average 34.1% within realigned reaches with a range of 15.8% - 45.3% (Table 5). In the non-realigned reach the average value was found to be 33.1% with a range of 25.5% - 40.7%. The similarity in values may be due to the values for the SB2 reach being considerably lower than that of the other realigned reaches. (Table 5 and Table 6).

Storage zone exchange flux (qs) was found to be $0.007 \text{ m}^3\text{s}^{-1}\text{m}^{-1}$ within realigned reaches with a range of $0.004 \text{ m}^3\text{s}^{-1}\text{m}^{-1}$ – $0.012 \text{ m}^3\text{s}^{-1}\text{m}^{-1}$. The non-realigned reach was found to have an average value of $0.004 \text{ m}^3\text{s}^{-1}\text{m}^{-1}$ and a range of $0.003 \text{ m}^3\text{s}^{-1}\text{m}^{-1}$ – $0.006 \text{ m}^3\text{s}^{-1}\text{m}^{-1}$.

Hydrologic retention factor (Rh) was found to be 0.97 sm^{-1} in realigned reaches with a range of 0.056 sm^{-1} – 1.39 sm^{-1} . Whereas the mean hydrologic retention factor for non-realigned reaches is 0.84 sm^{-1} with a range of 0.67 sm^{-1} – 0.98 sm^{-1} . The value for SB3 2016 was removed from the mean calculation as it uses the TimeStor metric in the Rh calculation.

Restored Metrics							
Reach	Dal	Fmed@200 [%]	TimeStor [s]	Ls [m]	TranStor [%]	qs [$m^3s^{-1}m^{-1}$]	Rh [sm^{-1}]
SB1 2016	11.534	24.729	52.028	53.401	33.919	0.009	0.974
SB1 2017	7.543	29.651	71.670	66.328	45.307	0.008	1.081
SB2 2016	12.347	11.891	57.623	97.381	15.795	0.004	0.592
SB2 2017	13.475	19.882	50.050	59.134	25.915	0.012	0.846
SB3 2016	3.657	26.764	243.672	95.768	43.986	0.004	2.544
SB3 2017	5.837	26.843	90.807	65.120	39.175	0.007	1.394
Means	9.066	23.294	64.436	72.855	34.016	0.007	0.977

Table 5: Metrics used in this study to quantify transient storage in the Realigned Reaches. Dal = Damköhler Number, FMed@200 = Median Travel Time due to Storage in a 200m Reach, TimeStor = Residence Time in Storage, Ls = Storage zone Turnover Length, TranStor = Transient Storage %, qs = Storage Zone Exchange Flux, Rh = Hydrologic Retention Factor. The SB3 2016 TimeStor reading was removed due to being an outlier. Due to Rh being calculated using TimeStor, this metric was also omitted from the mean calculation (in this table it has been crossed out for transparency).

Unrestored Metrics							
Reach	Dal	Fmed@200 [%]	TimeStor [s]	Ls [m]	TranStor [%]	qs [$m^3s^{-1}m^{-1}$]	Rh [sm^{-1}]
SB4 2016	4.841	17.104	75.847	108.698	25.523	0.003	0.698
SB4 2017	4.717	26.663	76.765	78.429	40.689	0.006	0.979
Means	4.779	21.883	76.306	93.563	33.106	0.004	0.838

Table 6: Metrics used in this study to quantify transient storage in the non-realigned reaches

Figure 10 illustrates the difference in calculated parameters between the realigned and non-realigned reaches in the form of box and whisker plots. All of the metrics show a greater range of values in the realigned reaches than the non-realigned reaches partially due to the larger number of realigned reaches compared to the non-realigned reach. Ls and TimeStor are the only metrics where the average value is higher in the non-realigned reach compared to the realigned reaches. The skew of plots also indicates the lack of normality that was found by the parametric tests.

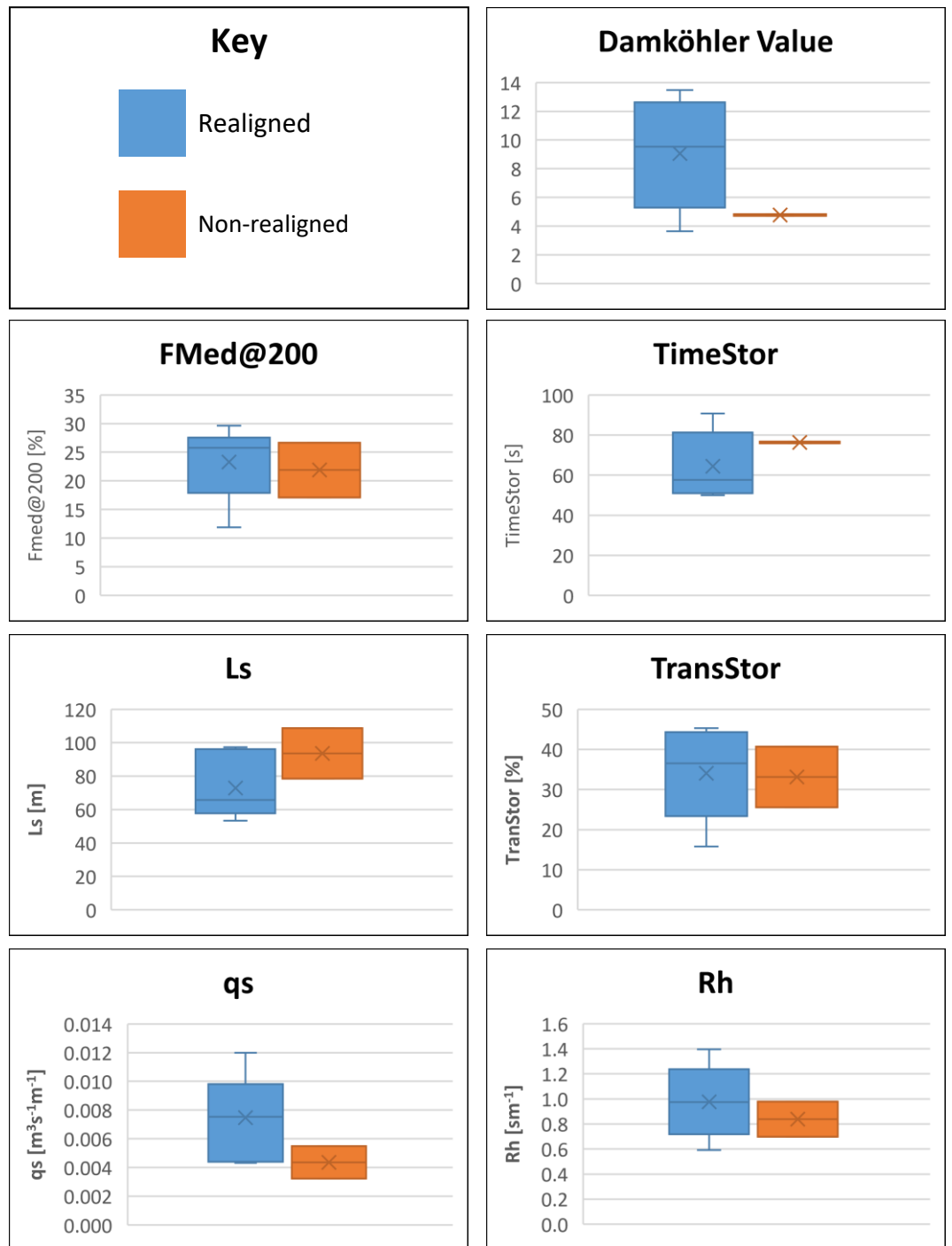


Figure 10: Box and whisker Plots to visualise the data displayed in Table 5 and Table 6. Note the lack of data from SB3 2016 TimeStor and Rh due to being considered anomalous.

4.3 Geomorphic Unit Analysis

UAV derived photogrammetry from 2016 and 2017 was analysed using the ArcGIS software to develop cross sections of each reach, planform elevation, and to quantify the area of geomorphic units in realigned reaches. This analysis was proofed by undertaking a reach survey for each of the four reaches. This survey was based on the stream reconnaissance handbook (Thorne, 1998) and used the Wentworth grain size classification (Wentworth, 1922). This can be seen in Table

18 within the Appendix. This analysis indicates that there was a greater number of riffles sandbars, and pools in the realigned reaches during 2017 compared to 2016 (Table 7). This finding was expected, as restoration had provided realigned with a wider river planform and variation in terms of meanders and river depth (Table 18), facilitating conditions needed for the formation and growth of bars, riffles and sand bars. The greater overall area of each geomorphic unit is a good indicator of the river returning to its natural dynamic equilibrium (Woolsey et al., 2007). However, only the larger area for the sandbars was calculated to be statically significant while the larger area for the pools and riffles was not statically significant.

The variation in average bank slope angle is evident in Table 18 with the non-realigned reach SB4 having the steepest average bank slope angle (90 Degrees) when compared the realigned reaches SB1, SB2, and SB3. This was due to the bank reinforcement that was in place to prevent lateral erosion. This meant that there was less erosion within this reach and this is clear in Table 18. The SB2 left bank was also very steep at 90 Degrees; this was potentially caused by this area being most active in terms of erosion (Table 18). The river reach survey highlighted that the realigned reaches show signs of localised mild erosion (Table 18), whereas, the non-realigned reaches did not due to the reinforced banks. The main erosive processes found within the realigned reaches were parallel flow with some small-localised impinging flow caused by larger riffles. This increase in parallel flow and lack of bank reinforcement has led to the formation of a much wider lateral extent in the realigned reaches as opposed to the non-realigned reaches. The vegetation was similar across all four reaches, with the exception being the trees planted at the SB3 reach to stabilise the bank and to alleviate the pooling of surface water (Table 18). The banks of the Swindale Beck consists of a cohesive mixture of silt and clay with the non-realigned reaches and some sections of the realigned reaches being reinforced with boulders from the channel (Table 18). In the case of the SB3 reach, this was to prevent the river from returning to the pre-realigned channel. Each of the reaches have very similar bank face vegetation consisting mainly of grass with the SB3 reach also containing riparian vegetation.

Figure 11 shows the downstream change in elevation along the study reaches in the Swindale Beck. Tree cover, which extended across the channel at the upper section of the SB3 reach, meant that the elevation was recorded as 5-10 metres higher than surrounding river elevation and was removed. The gap that was left is clear in Figure 11 at around 300 metres. The troughs located in the SB3 reach after SB2 and before SB1 was due to a deep pool in the river. The change in gradient is greatest in the non-realigned reaches SB4 and SB3, with SB2 having the lowest gradient.

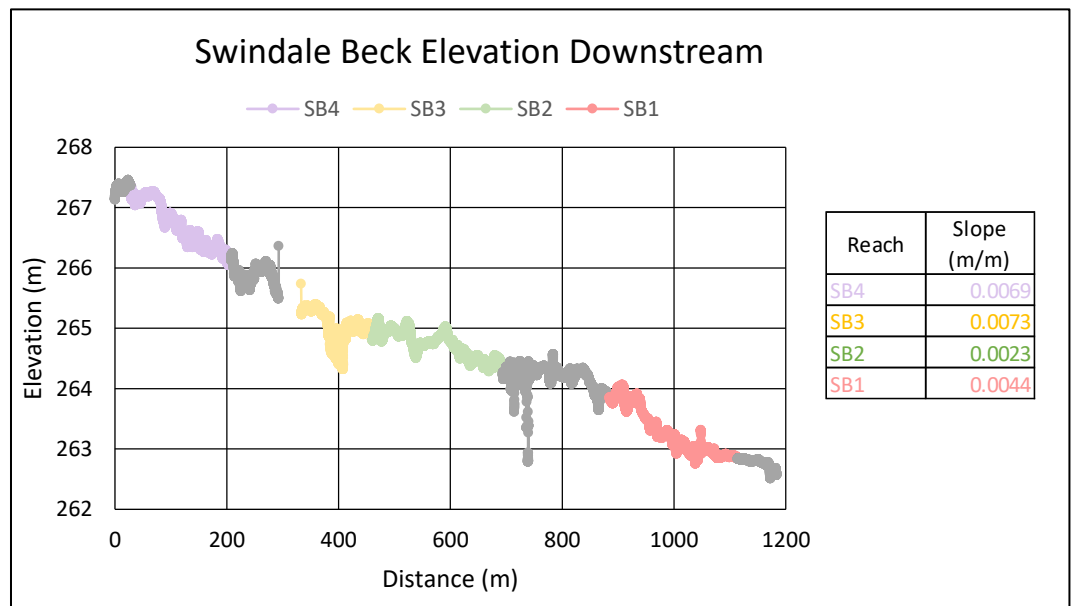
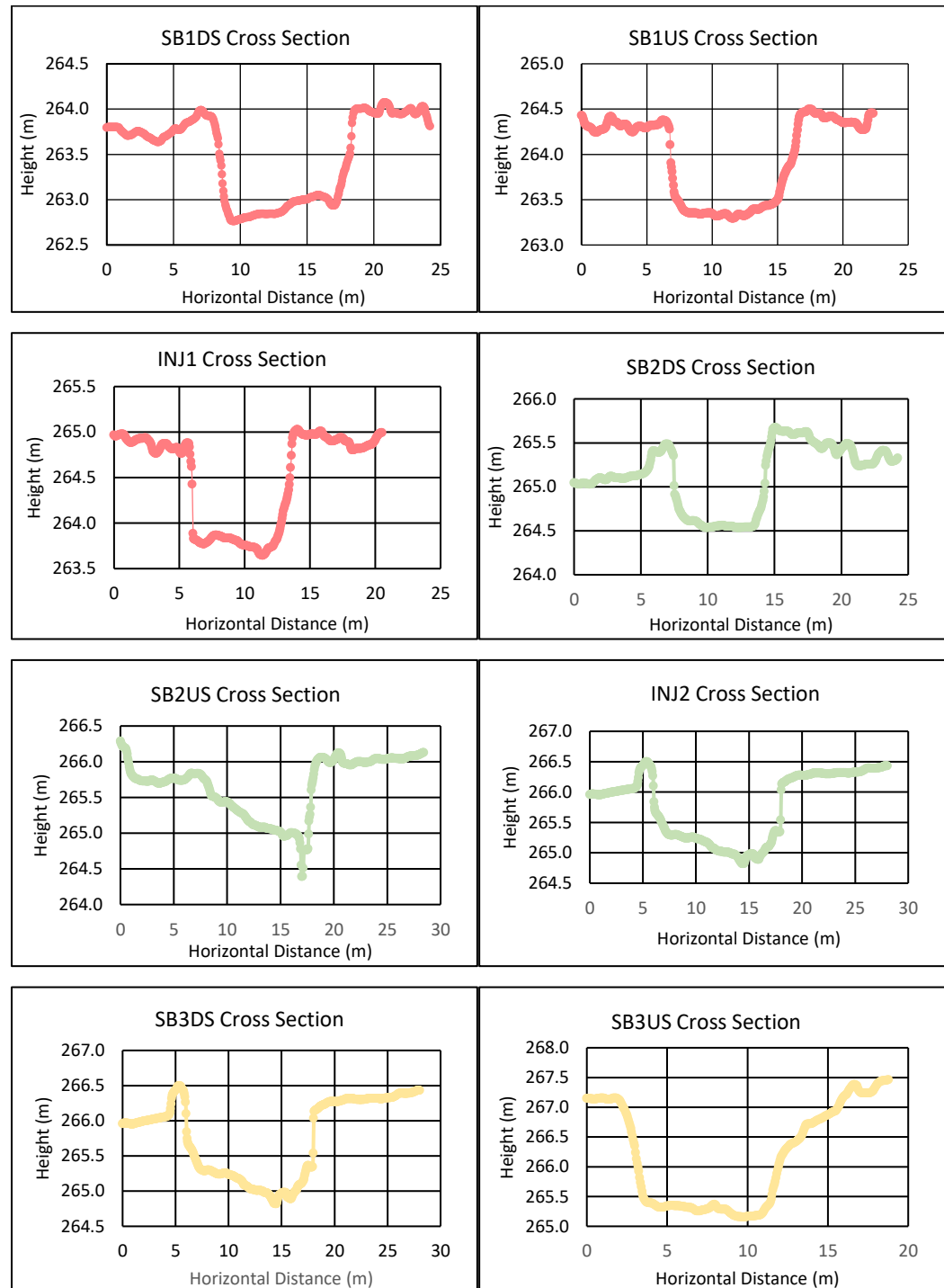


Figure 11: Downstream Elevation graph of the Swindale Beck. The grey areas are areas of the Swindale Beck that were not located within the study reaches. The gap at the start of the SB3 reach can be clearly seen and is caused by the deletion of inaccurate elevation data caused by tree cover.

Figure 12 illustrates the cross-sections that were calculated at the injection site (INJ) the upstream monitoring site (US) and the downstream monitoring site (DS) for each reach studied of the Swindale Beck. It is clear that the non-realigned reach SB4 has much steeper banks and a much narrower channel bed than the realigned reaches. This call is also evident in the River Reach Survey (Table 18). The cross-section of the SB4 reach clearly illustrates the uniform channel in addition to the levees built by the landowner. The average width of the channel at bank full increases from SB1 to SB4, with SB1 reaches being the widest and SB4 being the thinnest. The average depth at bankfull for all four reaches was found to be between 1.0 metres and 1.5 metres with an average of 1.1 metres. The depth of the river at bankfull was similar across all reaches except SB2, which was 25% lower than the average of 1.1 metres. The depth measurement was taken at bankfull, this was because the UAV photogrammetry was unable to detect the

height of the water within the channel due the limitations of UAV sensor not being water penetrating (Williams et al., 2014). Figure 12 shows the decrease in riverbed elevation by the decreasing minimum height of the channel in each cross-section from upstream to downstream (SB4 to SB1). The reach with the lowest slope in Figure 11 was SB3, this can be easily seen in Figure 12 when comparing the elevation of the riverbed at SB2US and SB2DS.



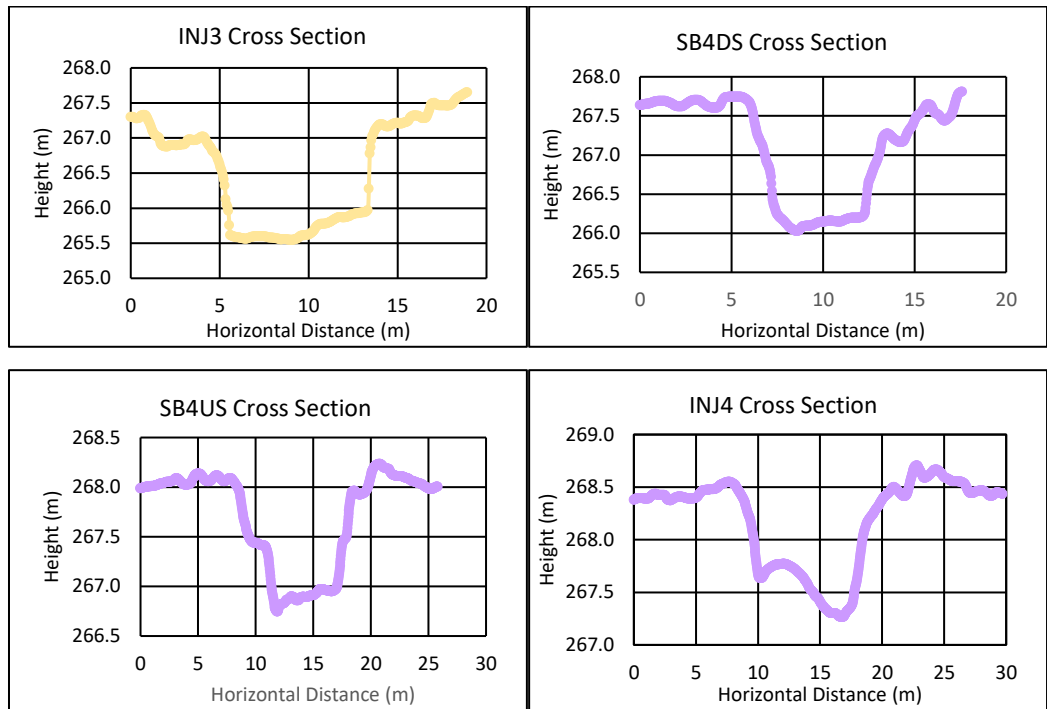


Figure 12: Representative cross-sections of each of the sample locations. Note that SB3DS and INJ2 are nearly identical due to being located at the same location.

Data collected from digitising geomorphological features such as, riffles, pools, and sandbars in ArcGIS shows that there is a greater area for all three features, 27%, 39% and 15% respectively in 2017 than in 2016 (Table 7). These features were selected as they are recommended by Thorne (1998). In addition, they are easy to identify from the drone images and thus can be straightforwardly digitised.

Geomorphic Unit Analysis (Restored Reaches Only)				
Year	Riffles Area [m ²]	Pools Area [m ²]	Sandbars Area [m ²]	Total Area [m ²]
2016	350.77	158.97	1268.53	1778.27
2017	481.29	262.81	1506.37	2250.47
Percentage Increase [%]	37.21%	65.32%	18.75%	26.55%

Table 7: Table showing the change in area for riffles, pools, and sandbars. The table also displays the percentage change since the previous year. Pools area shows the greatest overall change at 39.51% whereas sandbars shows the smallest change of 15.79

There was a statistically significant change ($p < 0.01$) in the area of sandbars (1268.53m² to 1506.37m²) in the Swindale Beck from 2016 to 2017. There was no statistically significant change ($p > 0.01$) in the size of riffles (350.77m² to 481.29m²) and in pools (158.97m² to 262.81m²) in the Swindale Beck from 2016 to 2017. Unfortunately, only the realigned reaches SB1, SB2, and SB3 are included, as the UAV derived photogrammetry did not encompass the SB4 reach during data collection in 2017.

5.0 Discussion

5.1 Spatial and Temporal Patterns in Transient Storage

5.1.1 Damköhler Number

The realigned reaches SB2 and SB3, both experienced a higher Damköhler number during 2017 compared to 2016. Whereas, the realigned reach, SB1, and the non-realigned reach, SB4, experienced a lower Damköhler number in 2017 compared to 2016. The average Damköhler number is highest in realigned reaches, being 89% larger than that of the non-realigned reaches. The higher Damköhler number implies that the tracer in the realigned reaches underwent less effective mixing than that of tracer in the non-realigned reaches. This is most likely due to the boulder steps that are present within the non-realigned reaches which would aid in mixing due to the increased downwelling and subsequent water turbulence. This contrasts with the realigned reaches, which although having vastly more geomorphological features (riffles, pools, and sandbars), do not have any features which are as effective at mixing as the boulder steps located in the non-realigned reach. Despite the higher Damköhler value found in the realigned reaches, the values found in this study were close to the ideal range proposed by Harvey and Wagner (2000), indicating that the reach lengths were acceptable for the OTIS Model, and that this study is confident in the calculated parameter estimates. However, the study by Knust and Warwick (2009) calculated the Damköhler number to be above 1000, indicating significant uncertainties in their parameter estimates. Wagner and Harvey (1997) suggest that this is due to the reach being too long and the majority of the tracer is exchanged with the storage zone before the sampling location.

5.1.2 FMed@200

FMed@200 is the fraction of the median reach travel time due to storage. In effect, this metric is the percentage of the median travel time due to the temporary retention of water in transient storage zones. This metric allows for effective comparisons between reaches of different lengths as the length of the reach is standardized to 200 metres during the metric calculation. In this study, it is clear that FMed@200 is slightly higher in 2017 than in 2016 in all reaches, with the average value for the realigned reaches being 6% larger than the average for

the non-realigned reaches. This would imply that the influence of transient storage on travel time is very similar in both realigned and non-realigned reaches.

SB2 shows the lowest FMed@200 values within realigned reaches, indicating a low median travel time due to transient storage. This could potentially indicate a lower magnitude of transient storage compared to the other reaches and may be caused by the low slope of the reach impeding hydraulic head gradients, and subsequently, subsurface transient storage (Figure 11). It was discovered while calculating the OTIS parameters for the SB2 reach, that the discharge for this reach during 2017 was higher than expected. This was suspected to be caused by a large pool downstream of the injection site, potentially acting as a storage zone for the tracer. However, this value was not anomalous enough to be considered an outlier. This uncertainty is evident in the breakthrough curve for SB2 2017 as the simulated breakthrough curve is lower than the observed breakthrough curve. It is clear that the FMed@200 percentage was higher in every reach during 2017 compared to 2016. The greatest percentage change occurred in the realigned reach SB2, which experienced a value 67% greater during 2017 than found during 2016.

FMed@200 has been found to decrease as water velocity increases (Runkel, 2002, Stofleth et al., 2008, Marttila et al., 2018). Conversely, Roberts et al. (2007) found that in realigned reaches FMed@200 increased with water velocity. Mason et al. (2012) also found similar results with restoration increasing residence time within the channel; this was attributed to a decrease in channel slope and an increase in pools. Bukaveckas (2007) discovered that FMed@200 was 50% greater in realigned reaches than non-realigned reaches; this was attributed to a decreased velocity and an increase in the meandering channel length. In this study, FMed@200 percentage was higher in every reach during 2017 compared to 2016; the two reaches that saw the largest change in FMed@200 from 2016 to 2017 were SB4 and SB2. The two reaches with the lowest change in FMed@200 from 2016 to 2017 were SB3 and SB1. Within the realigned reaches, the reaches with the lowest slope (SB1 and SB2) experienced a much greater change in FMed@200 from 2016 to 2017. The realigned reach with the highest slope (SB3) saw the smallest change in FMed@200 from 2016 to 2017. The potential relationship between the slope of the reach and FMed@200 is similar to that explained by

Mason et al. (2012) who attributed increases in FMed@200 to be linked to an increased slope angle. Kupilas (2017) observed that realigned reaches experienced lower velocity and an increase in FMed@200 compared to non-realigned reaches. It was suggested that this was caused by the increase in morphological features including islands and macrophyte patches. In this study, realigned reaches have a lower average velocity but only have a slightly lower average FMed@200 value. Mueller Price et al. (2016) found that FMed@200 was lower in reaches with lower discharges. This study found that reaches with the greatest increase in FMed@200 also had the lowest change in discharge from 2016 to 2017. This implies that reaches where the discharge did not vary greatly from 2016 to 2017, experienced an increase in the average amount of time water spends within the storage zone.

5.1.3 Residence Time in the Transient Storage Zone (TimeStor)

Residence time in storage (TimeStor) initially indicated a shorter residence time within the transient storage zones of non-realigned reaches compared to realigned reaches. However, this was due to the anomalous value calculated for the SB3 reach which was removed, leading to a lower average TimeStor value in realigned reaches. This was believed to be caused by an unusually large main channel storage area being calculated by the OTIS-P model within the SB3 reach during 2016, which was not observed in subsequent years. Removing SB3 2016 TimeStor value from the mean calculation alters the mean value from a 24% higher average value in realigned reaches, to a 30% lower average value in realigned reaches. Implying that the solute was spending less time in the storage zone within the realigned reaches.

The SB1 reach shows the largest increase in TimeStor values from 2016 to 2017 compared the non-realigned reach SB4, which only showed a small increase in TimeStor values during the same period. Despite being realigned at the same time as the SB1 reach, the SB2 reach shows a lower value for the residence time within the storage zone during 2017 than during 2016. This lower residence time in storage was due to the OTIS-P model calculating a greater main channel storage area during 2017 compared to 2016, resulting in a lower residence time in storage value. The lower average residence time spent by water within the storage zone is less in the realigned reaches in comparison to the non-realigned reaches. This suggests that exchange is taking place more rapidly within the realigned reaches.

Becker et al. (2013) and Bukaveckas (2007) observed lower residence time in storage in realigned reaches compared to non-realigned reaches. This was linked to the heavy machinery, which worked within the dry realigned river channel. The led to the compaction of the channel bed and reduced the presence of hyporheic flowpaths within the subsurface, causing a reduction in residence time.

5.1.4 Storage Zone Turnover Length (L_s)

Storage zone turnover length (L_s) describes the distance that water travels within the storage zone. Results from this study indicate that the distance that water travelled within the storage zone was 22% less within the realigned reaches in comparison to the non-realigned reaches. Implying that exchange within the storage zone of realigned reaches is occurring more frequently than within the storage zone of the non-realigned reaches. Furthermore, this suggests that the storage zone of the realigned reaches may be dominated by rapidly exchanging surface storage as opposed to the much slower subsurface storage present in the non-realigned reaches.

5.1.5 Standardised Storage Zone Area (TranStor)

The standardised storage zone area (TranStor) was 3% larger in the realigned reaches in contrast to the non-realigned reaches. Only the realigned reach, SB1, experienced a lower TranStor value during 2017 than during 2016. This implies that the overall percentage area of the channel, that is storage zone, did not vary greatly from 2016 to 2017.

5.1.7 Storage Zone Exchange Flux (q_s)

The storage zone exchange flux (q_s) was 71% larger in realigned reaches compared to non-realigned reaches. SB1 was the only reach that showed a lower value for q_s during 2017 compared to 2016. This was due to the OTIS-P model calculating a lower value for the 'main channel storage area' for SB1 2017, which led to a greater storage zone exchange flux value for the SB1 reach. The results suggest that more water was travelling through the storage zone per unit area. This data can be interpreted that there was a higher exchange rate between surface water and the storage zone within realigned reaches.

5.1.8 Hydrologic Retention Factor (Rh)

The hydrologic retention factor (Rh) was 16% higher in realigned reaches compared to the non-realigned reach. This would imply that water is spending more time within the surface per metre of the reach before entering the storage zone. Further suggesting that water is travelling a shorter distance, exchanging more rapidly and spending a shorter amount of time within the with the storage zone within the realigned reaches.

5.2 Summary of Metrics

The transient storage metrics used in this study indicate fundamental differences in the transient storage mechanisms that govern realigned and non-realigned reaches. The lower residence time in storage (TimeStor) in realigned reaches indicated that water spent less time within the storage zone compared to the non-realigned reach. The greater storage zone exchange flux (q_s) indicated that more water flowed through the storage zone per unit area within the realigned reaches compared to the non-realigned reach. This constitutes to a higher exchange rate between the channel and the storage zone. The lower storage zone turnover length (L_s) value indicated that the distance that water travelled within the storage zone was less within the realigned reaches in comparison to the non-realigned reach. The greater hydrologic retention factor (Rh) within realigned reaches shows that the channel water was spending longer within the surface waters of the channel before being exchanged with the storage zone. This would suggest that the realigned reaches were dominated by rapidly exchanging surface transient storage with much less surface-subsurface interaction than that of the non-realigned reaches. The prevalence of surface storage was likely caused by decreased hydraulic head gradients in realigned reaches further due to a lack of irregularity within the channel. This subsequently led to reduced hyporheic flow and reduced subsurface storage (Harvey and Bencala, 1993, Wörman et al., 2002, Ensign and Doyle, 2005, Wondzell, 2006, Mason et al., 2012, Weigelhofer, 2017, Ward et al., 2018). The reduction in the slope of the realigned reaches may have also contributed to a decrease in hydraulic head (Mason et al., 2012).

Several other studies have also used a solute tracer injection to determine the impact of river restoration on transient storage. Bukaveckas (2007) used a transient storage model to quantify the effects of channel restoration on transient

storage. The restoration efforts included: reconnecting the previously canalised channel to its floodplain, reintroducing channel meanders, and pool and riffle features to provide a variety of flow conditions within the channel. The study described an overall increase in median travel times (FMed@200) within the realigned reaches compared to the previously non-realigned channel. This was attributed to the increase in the length of the meandering channel and the decrease in velocity.

Conversely, a study by Becker et al. (2013) exemplified an overall increase in median travel times (FMed@200) within the non-realigned reaches. This contrasts the findings of this research where median travel times (FMed@200) were similar in both realigned and non-realigned reaches. The results of this study demonstrated evidence similar to Becker et al. (2013), where the OTIS model was used to quantify the impacts of channel restoration on transient storage using a conservative tracer. However, the methodology conducted by Becker et al. (2013) differed from that used by Bukaveckas (2007) as the former focused on the use of river steering structures to reduce erosion and facilitate pool formation instead of decreasing the slope of the channel. The study by Becker et al. (2013) found a lower value for storage zone turnover length (Ls) and residence time within the storage zone (TimeStor) within realigned reaches; alongside an increase in the storage zone exchange flux (qs), and hydrologic retention factor (Rh). This was further interpreted that the realigned reaches were dominated by fast in-channel surface storage, whereas, the non-realigned reaches were characterised by much slower exchange. These results and interpretations were profoundly similar to this study. The comparative results of Bukaveckas (2007) and Becker et al. (2013) were described explained by the use of river steering structures within the channel by the latter study. These river steering structures were described to be very similar in characteristics to river drop structures (Figure 13a), inducing downwelling into the subsurface and producing eddy currents (Becker et al., 2013). However, compaction from heavy machinery acted to reduce the surface-subsurface interaction caused by the downwelling (Figure 13b).

Rana et al. (2017) used a solute tracer in conjunction with the OTIS and OTIS-P models to quantify transport parameters (the model parameters used in this study) but did not calculate metrics of transient storage. The study found that

transient storage increased with increasing numbers of channel structures but also found a decrease in the transient storage exchange rate. This was attributed to slow moving hydrostatically driven subsurface storage being induced behind the channel structures. This contrasts with the results of this study which found rapidly exchanging surface storage due to a lack of channel structures.

5.3 Conceptual Model of Transient Storage

Figure 13a illustrates the processes that were hypothesised to be occurring at the boulder steps within the non-realigned reach, SB4. The hydraulic gradient across the boulder step forces the water upstream of the step into the hyporheic zone and drives water from the hyporheic zone into the water column where it travels to the topographic low of the bed form causing an area of upwelling (Figure 13a; (Harvey and Bencala, 1993, Wondzell and Swanson, 1999, Boulton, 2007). Surface water that passes into the hyporheic zone will provide the hyporheic zone with both nutrients and dissolved oxygen from the water column (McLachlan et al., 1990), enabling biological and geochemical processes to take place. However, not all of the water will be able to travel through the channel bed and some will be deflected laterally; this leads to the formation of an eddy current at the base of the boulder step. The prevalence of eddy currents in the non-realigned reach is potentially the reason for better mixing and the subsequent lower Damköhler values found within the non-realigned reach compared to the realigned reaches (Table 5 and Table 6). The combination of eddy currents, areas of downwelling, and subsequent subsurface flowpaths may attribute to the 22% shorter storage zone length (L_s) in realigned reaches. This would imply that the subsurface flowpaths within the non-realigned reach were greater in length than the surface storage zones within the realigned reaches. Figure 13b illustrates how within the realigned reaches, the lack of channel structures and subsequent lack of localised hydraulic gradients led to a decrease in surface-subsurface interactions. The 16% greater hydrologic retention factor value (R_h) in the realigned reaches implied that water within the channel was travelling further per metre before being exchanged with the storage zone. This may be due to the decrease in surface-subsurface interactions within the realigned reaches by the marginally higher median travel times due to storage ($F_{Med@200}$) caused by an increase in meandering channel length (Figure 15). Decreased surface-subsurface interactions within the realigned

reaches may have also been caused by the compaction of the channel bed and the subsequent pore space clogging by the use of heavy machinery within the channel during restoration, further limiting vertical connectivity (Figure 13b) (Wörman et al., 2002, Mason et al., 2012, Weigelhofer, 2017). Moreover, this could result in a decrease in the number of surface-subsurface pathways (which can be seen by the smaller subsurface flow arrow in Figure 13b compared to Figure 13a), causing the channel water to travel further before entering the storage zone (Rh). Bukaveckas (2007) and Becker et al. (2013) also referred to this phenomenon occurring during their studies. The lack of channel irregularities to induce downwelling, and the compaction of the channel bed, implies that the storage zone within the realigned reaches consists primarily of surface storage that was exchanging rapidly with the water column (qs) and, thus, spending less time within the storage zone (Timestor). The lack of subsurface flowpaths and the greater mean travel times due to storage (FMed@200) meant that water had to travel further before entering the storage zone (Rh), suggesting that the realigned reaches were dominated by rapidly exchanging surface storage.

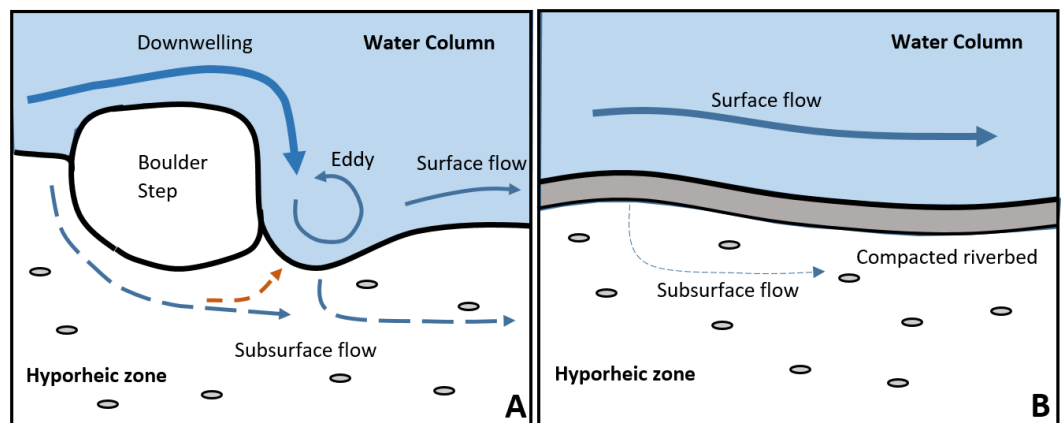


Figure 13: Longitudinal conceptual model illustrating the impact of streambed topology on subsurface flow and hyporheic exchange. Image A is the non-realigned reach, SB4, containing boulder steps. Image B is the realigned reaches SB1, SB2, and SB3, which lack such structures. The boulder steps lead to increased surface-subsurface exchange within the non-realigned reaches, which was less prevalent within the realigned reaches. The thickness of the arrows represents magnitude of flow. The solid arrow represents surface channel flow, whereas, the dotted arrow represents subsurface flow. The orange arrow indicates areas of upwelling.

There is the possibility that the restriction of surface-subsurface flowpaths may not be exclusively caused by the compaction of the riverbed. Pore space clogging potentially caused by clay and other small particulates may lead to a decrease in surface-subsurface interactions (Kasahara and Hill, 2006, Packman and MacKay, 2003). (Packman and MacKay, 2003). Packman and MacKay (2003) found that even small amounts of clay were enough to cause significant clogging of the

riverbed. Another potential cause for decrease surface-subsurface flowpaths may be the presence of a layer of clay below the bed of the channel, inhibiting the movement of water through it. Boulder clay is a typical glacial deposit and given that the valley most likely experienced glacial processes during the Younger Dryas, the formation and deposition of boulder clay is possible (Brown et al., 2011). A further potential cause for the decreased surface-subsurface interactions could be caused by the bedrock of the valley being located close to the bed of the channel inhibiting the flow of water downwards. These potential causes of the low surface-subsurface interaction should be further examined in future studies within the Swindale Beck.

The greater number of riffles and sandbars (Table 7) within the realigned channel could potentially lead to an increased number of surface-subsurface interactions. Similarly to the boulder steps (Figure 13), the riffles (Figure 14a) and the sandbars (Figure 14b) form a hydraulic gradient. However, due to the smaller elevation change the hydraulic gradient would be less than that found across the boulder steps. The hydraulic gradient forces water through the riffles and sandbars where it travels to the topographic low, forming an area of upwelling, and provides a localised concentrated surface-subsurface interaction (Figure 14a) (Endreny et al., 2011, Gariglio et al., 2013). Because riffles and sandbars are present within the realigned reaches, this would imply that the reaches do not only consist of surface transient storage, but do in fact contain low levels of subsurface transient storage. However, the magnitude of surface-subsurface exchange caused by sandbars and riffles would be less than that produced by the boulder steps. This was evident by the hydrologic retention factor (R_h), as water within the realigned channel takes 16% longer to enter the storage zone per metre of channel. Potentially, less water could travel into the subsurface because the riffles and sandbars are less effective at inducing surface-subsurface interactions than the boulder steps (Hester and Doyle, 2008, Gariglio et al., 2013). One of the biggest difference between riffles and sandbars is the grainsize and pore spaces. The smaller grainsize of the sand (Figure 14b), compared to the cobbles and boulders in the riffle (Figure 14a), decrease the magnitude of surface-subsurface interaction due to the restriction a smaller grainsize has on fluvial flow (Findlay, 1995, Packman and Salehin, 2003, Boulton et al., 2010). The fact that sandbars do not span the entire channel also

decreases the magnitude of surface-subsurface interaction (Hester and Doyle, 2008). This process is similar to the downwelling process in Figure 13 but on a much smaller scale. The larger grain sizes of the pebbles, compared to the sand, cause a greater disruption of flow leading to increased pressure variations and to increased surface-subsurface interactions (Elliott and Brooks, 1997, Cardenas et al., 2004). The 22% lower storage zone length (L_s), alongside the 30% lower residence time within the storage zone (TimeStor) in realigned reaches, may be partially influenced by the magnitude of surface-subsurface interaction induced by the riffles and sandbars, which is lower than that induced by the boulder steps. The overall result could lead to a smaller length of the storage zone and a reduced residence time in storage within the realigned reaches.

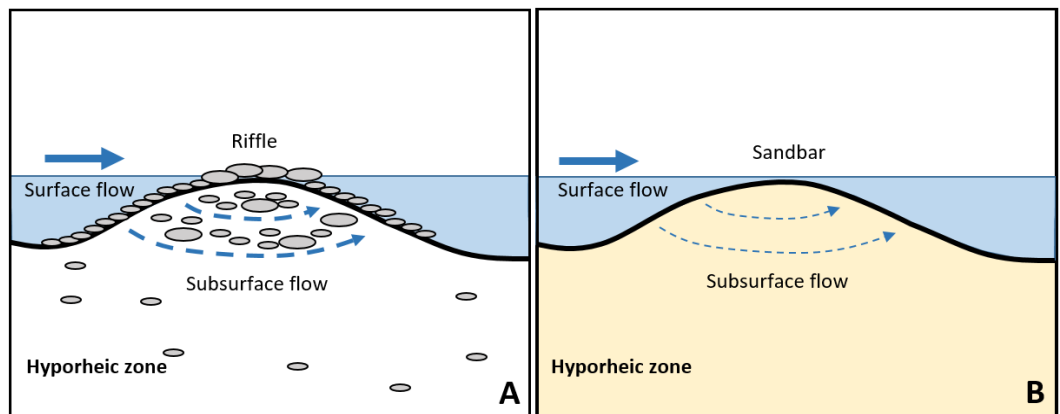


Figure 14: Longitudinal conceptual model illustrating the impact of riffle (A) and Sandbar (B) on subsurface flow and hyporheic exchange. The grey ovals represent pebbles/cobbles/boulders with large pore spaces within the riffle. The yellow background of the sandbar represents the sand with very small pore spaces. The solid arrow represents surface channel flow whereas the dotted arrow represents subsurface flow. Like Fig 12, the thickness of the arrows represent the magnitude of flow.

The greater mean travel times due to storage (FMed@200) in realigned reaches was potentially caused by the increase in length of the meandering channel and the decrease in velocity in realigned reaches. The increase in meandering channel length may cause lateral exchange of surface water through saturated sediments (Figure 15), (Findlay, 1995). This process would be more prevalent in reaches with higher hydraulic head gradients, allowing the water to pass more easily through the pore spaces in the meander neck (Boano et al., 2006). Increased meander length and decreased width of the meander neck increases the amount of water passing laterally through the meander (Boano et al., 2006). In the case of the Swindale Beck, the non-realigned reach (Figure 15a) contains few meanders alongside the reinforced banks preventing the lateral movement of water into the

subsurface. In contrast, the lack of bank reinforcement and the multitude of meanders within the realigned reaches (Figure 15b) allows for lateral surface-subsurface interaction to occur. The fact that the realigned meanders were constructed with heavy machinery would affect the rate at which lateral surface-subsurface exchange occurs until the compacted surfaces are eroded and pore spaces are reopened. This speculated to be the the reason why the realigned reaches are surface storage dominated despite having an increase in the number of meanders and the removal of the reinforced banks (Figure 15). Despite the increase in channel length, the storage zone length (L_s) was lower in realigned reaches. This would imply that the length of the subsurface flowpaths and subsequent storage zones within the non-realigned reach are greater in length than the surface storage zones found in the realigned reaches. The larger storage zone exchange flux (q_s) within realigned reaches implies that despite being shorter in length, the storage zones are larger in volume within the realigned reach. More water per unit area would be able to travel through storage zones per second in realigned reaches than the storage zones located within the non-realigned reach, because discharges within both realigned and non-realigned reaches are similar.

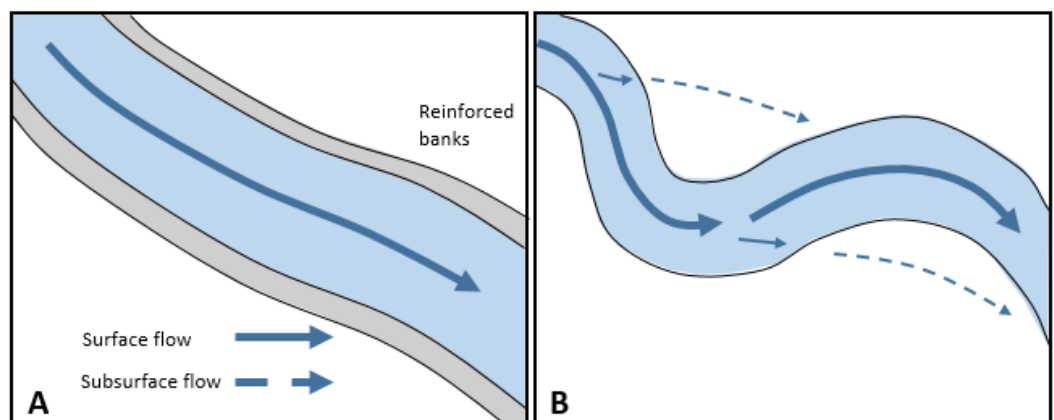


Figure 15: Planform conceptual model illustrating the impact of channel meandering on lateral surface-subsurface exchange. Image A is the non-realigned reach SB4 containing few meanders. Image B is the realigned reaches SB1, SB2, and SB3, which contain multiple meanders.

Figure 13 and Figure 14 illustrate some of the variations in surface-subsurface interactions within the realigned and non-realigned reaches. Surface-subsurface interaction found within the non-realigned reaches is driven by the downwelling from the boulder steps, driving water into the subsurface. Within the realigned reaches much less surface-subsurface interaction is occurring due to the compacted channel bed and the geomorphic features only inducing small-

localised areas of surface-subsurface interaction. Figure 16 illustrates the magnitude of surface-subsurface interactions within both the realigned and non-realigned reaches. Figure 16a illustrates the non-realigned reach, with the majority of surface-subsurface interaction (orange arrows) being caused by the boulder steps. The non-realigned reach also contains reinforced banks, which limit the access of the channel to the floodplain (green arrows), as well as preventing lateral surface-subsurface exchange (Figure 15), and natural channel progression. This is in contrast to the realigned channel (Figure 16b), where the reinforced banks have been removed, allowing the channel access to the floodplain, and facilitating lateral channel progression (green arrows) (Findlay, 1995). The reconnection of the channel to the floodplain, in addition to providing nutrients and organic matter, will increase the quantity of boulders and woody debris within the channel post flood event (Bukaveckas, 2007), thus increasing surface-subsurface interactions by facilitating the formation of hydraulic gradients (Figure 13). The formation of riffles, sandbars, and pools, will also induce surface-subsurface exchange (Kasahara and Wondzell, 2003). However, as illustrated in Figure 16, and as shown by the metrics used in this study, these geomorphic features will not be as effective at inducing surface-subsurface interactions than the boulder steps located within the non-realigned reach (Hester and Doyle, 2008, Gariglio et al., 2013). The higher Damköhler number within the non-realigned reach implies that the boulder steps are more effective at mixing channel water than the geomorphic units present within the realigned reaches. Pools within the realigned reaches do not have the increased hydraulic head gradients caused by the boulder steps, suggesting that the pools and boulder steps are a driver for surface-subsurface interactions, whereas, the pools located in the realigned reach are surface storage zones, with much less surface subsurface interaction. The surface-subsurface interaction induced by the riffles is larger than that induced by the sandbars due to the larger grain sizes found within the riffles creating an increased hydraulic gradient.

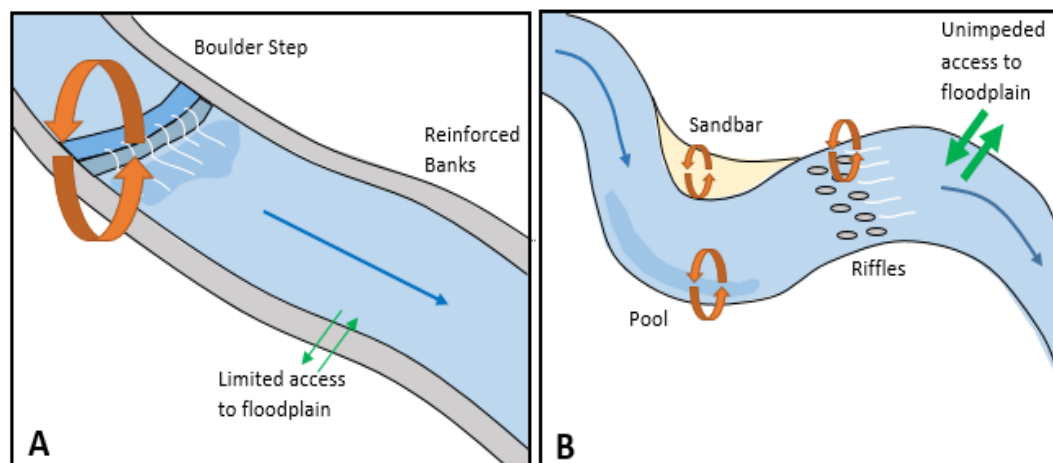


Figure 16: Planform conceptual model illustrating the impact of removing reinforced banks and allowing the channel to meander. Image A is the non-realigned reach SB4 containing boulder steps. Image B is the realigned reaches SB1, SB2, and SB3 containing more geomorphic units. The orange arrows indicate the surface-subsurface caused by each geomorphic feature. The green arrows illustrate the connectivity of the reach to the flood plain (bigger arrows means greater connectivity).

5.4 Implications for River Restoration

This research demonstrates how the restoration of a channel can affect surface-subsurface interactions. The metrics used in this study, in conjunction with the conceptual models, indicate that the restoration processes undertaken on the Swindale Beck led to the realigned reaches becoming a surface storage dominated system. This research has shed light on three key aspects which this study would advise to be considered in future river restoration schemes: riverbed/bank compaction, bank removal, and maximising surface-subsurface interactions.

This research has revealed that one of the key reasons that the realigned reaches are heavily dominated by surface transient storage is because of the compaction of the riverbed and riverbanks by heavy machinery during restoration (Figure 13 and Figure 16). This potentially led to a decrease in the number of surface-subsurface flowpaths as pore spaces were closed and this led to an increase in the distance that water travelled before entering the storage zone (R_h). Additionally, this further resulted in surface storage zones becoming dominant within the realigned reaches, as water exchanged rapidly with the surface storage zone (q_s) and less time spent within the storage zone (Timestor). A similar effect was also believed to have occurred during the removal of the reinforced banks which limited lateral surface-subsurface exchange and channel meandering. The metrics used in this study demonstrate that a potential decrease of pathways into the subsurface may lead to a reduction in the amount of water entering the hyporheic

zone (Rh, TimeStor), potentially leading to a decrease in exposure time of water with biogeochemically active surfaces within the storage zone. Further resulting in a decline in biogeochemical transformations (Bencala et al., 1984, Constantz, 1998, Harvey and Fuller, 1998, Duff and Triska, 1990, Hill et al., 1998, Jones Jr et al., 1995, McMahon and Böhlke, 1996). Few studies have looked at the effect of channel bed compaction and the underlying effect present on surface-subsurface interaction within realigned rivers and river restoration schemes. This study advises that the compaction of the riverbed/banks and the subsequent blocking of pore spaces and flowpaths should be minimised in order to ensure surface-subsurface interaction occurs within the realigned reaches.

The reconnection of a river to its floodplain was highlighted by Palmer et al. (2005) as one of the key natural river processes that must be undertaken in order for river restoration to be considered successful. River floodplains are very active biogeochemically (Tockner and Stanford, 2002, Baker and Vervier, 2004) and are second only to estuaries in terms of productivity and ecosystem services (Costanza et al., 1997). The removal of restrictions potentially has the largest effect on restoration, as it facilitates the progression of the channel back to a state of dynamic equilibrium, as unimpeded access to the floodplain will potentially provide the realigned channel with a source of nutrients, organic matter, and channel debris. Floodplain reconnection would help to alleviate the potential decrease of nutrients caused by the overall lower residence time with the storage zone (TimeStor) and greater in hydrologic retention factor (Rh) in realigned reaches. Realigned access to the floodplain will also have the effect of improved flood attenuation within the realigned reach (Sholtes and Doyle, 2010), minimising the effect of flooding further downstream. Furthermore, reconnection would also minimise the peak magnitude of flood events and decrease flood wave velocity within realigned reaches (Anderson et al., 2006, Dixon et al., 2016). Channel reconnection to the floodplain in conjunction to the introduction of riparian vegetation, will provide both a source of debris to the floodplain and river channel (Pess et al., 2005, Bukaveckas, 2007). The removal of the reinforced banks will also allow the channel to incise laterally as erosion would be able to occur upon the unprotected river banks. Potentially, this would lead to a more morphologically dynamic channel without compacted river banks or bed, leading to an increase in

surface-subsurface-interactions. However, the increase in riparian vegetation may reduce the erosive capacity of the channel upon the banks, potentially leading to increased erosion within the centre of the channel (Liu et al., 2017), negatively impacting the effect of restoration efforts.

This research would argue that the subsequent conceptual model has highlighted that re-establishing surface-subsurface interaction is of paramount importance with regards to successful channel restoration. The conceptual model (Figure 13 and Figure 16) indicates that the boulder steps facilitate the majority of the surface-subsurface interactions within the non-realigned reach. Whereas, within the realigned reach, riffles, sandbars, and pools facilitate the majority of surface-subsurface interactions (Figure 14 and Figure 16). The areas of downwelling and subsequent surface-subsurface interactions within the realigned reach were less significant than those found within the non-realigned reach. Areas of downwelling and transient storage have been linked to spawning locations of macroinvertebrates due to the constant temperatures and high levels of dissolved oxygen within the water (Findlay, 1995, Baxter and Hauer, 2000, Geist, 2000, Kondolf et al., 2008). Although not the focus of this study, the literature highlighted the importance of surface-subsurface interaction on riverine ecosystem health and subsequent ecosystem recovery (Findlay, 1995, Jones Jr et al., 1995, Riley and Fausch, 1995, Abbe and Montgomery, 1996, Brunke and Gonser, 1997, Hall et al., 2002, Bukaveckas, 2007, Baldigo et al., 2008, Miller et al., 2010, Argerich et al., 2011). However, the decrease of surface-subsurface interactions within realigned reaches could potentially lead to a decrease in nutrient cycling as less water being able to enter the subsurface and react with biogeochemically active surfaces (Bencala et al., 1984, Constantz, 1998, Harvey and Fuller, 1998, Duff and Triska, 1990, Hill et al., 1998, Jones Jr et al., 1995, McMahon and Böhlke, 1996). The important role of hydraulic gradients in facilitating the formation surface-subsurface interactions was emphasised in this study (Figure 13, Figure 14, and Figure 16). Hydraulic gradients could be induced with the introduction of in-channel debris such as woody debris or boulders within the channel (Gippel, 1995, Wörman et al., 2002, Binns, 2004, Kasahara and Hill, 2006, Mason et al., 2012, Wenzel et al., 2014, Weigelhofer, 2017), or by the formation of gravel beds within the river. These features would induce

downwelling similar to that illustrated in Figure 13 (Kurth et al., 2015). However, the removal of the reinforced banks and the subsequent floodplain reconnection could allow this process to occur naturally. Due to the lack of restriction, during flood events the channel would potentially be able to enter the floodplain to transport material into the channel, thus creating hydraulic gradients, and beginning the recovery of the surface-subsurface interactions within the realigned reaches. Thus, realigned reaches will potentially regain surface-subsurface interactions with given time as natural channel processes are now able to occur as man-made channel restrictions have been removed. Most significantly this research only describes the changes in transient storage from 2016-2017 and may not be indicative of long-term change.

6.0 Conclusions

The conclusions of this study are as follows:

1. Transient storage is understood to be an important metric to consider for ecosystem health. However, further research is required focusing on the impact that river restoration projects have on transient storage. This project highlighted the effectiveness of transient storage in determining the impact of river restoration schemes and supports recommendations into how river restoration could be implemented in the future.
2. This project used a conservative salt tracer and modelling approach to successfully quantify transient storage within realigned and non-realigned reaches of the Swindale Beck. The metrics of this study indicate that realigned reaches had a smaller storage zone length (L_s), a lower residence time within the storage zone (TimeStor), and a greater rate of exchange between the channel and storage zone (R_h) compared to the non-realigned reach. This heavily implies that reaches that underwent restoration became dominated by rapidly exchanging surface based transient storage as opposed to the non-realigned reach, which was dominated by subsurface transient storage.
3. The proposed conceptual model (Figure 13a), developed in this study demonstrates the effect restoration had on surface-subsurface interactions within the realigned reaches. From the conceptual model, it is evident that surface-subsurface interactions were induced by hydraulic

gradients forming across channel obstructions, which are not present in the realigned reaches.

4. The proposed conceptual model (Figure 13b), suggests that the compaction of the channel bed and riverbanks, due to restoration within realigned reaches of the Swindale Beck, may have decreased the number of surface-subsurface flowpaths. This potentially could have led to the lowered storage zone turnover length, storage zone residence time, and the higher in storage zone exchange flux and hydrologic retention factor within realigned reaches. The lack of surface-subsurface interactions within the realigned reaches may lead to a loss in habitat, spawning grounds, and a decrease in the subsurface reactions, subsequently leading to a decrease in channel productivity and recovery.
5. The removal of bank reinforcement (Figure 16) within realigned reaches during restoration will potentially allow the channel access to the biogeochemically active floodplain, and allow for lateral incision to occur. Floodplain access will also provide a source of nutrients, organic matter, and debris to the channel (woody debris and boulders). The increase in nutrients and organic matter may partially alleviate the effect that the decrease in surface-subsurface interactions had on biogeochemical cycling. The debris may facilitate in the recovery of surface-subsurface interactions within realigned reaches by inducing hydraulic gradients and areas of downwelling, providing habitat and enabling subsurface biogeochemical process to be realigned.
6. Of the three key aspects highlighted in this study that must be taken into consideration during river restoration, it is the removal of channel restrictions which is the most important to consider. This is because the removal of channel restrictions allow for natural river progression, erosion of the compacted banks and channel bed, and most significantly, the reintroduction of surface-subsurface interactions through the transport and deposition of floodplain debris.

7.0 Acknowledgements

Firstly, I would like to thank Dr Patrick Byrne, for his invaluable assistance during this project, including helping with data collection. I would also like to thank Dr Richard Williams for providing the UAV photogrammetry data of the site, and to Emanuele Chilleri and Courtney Carey for their assistance with data collection.

Secondly, I would like to thank the laboratory technicians Hazel Clarke and David Williams for their time and assistance with laboratory analysis and with help during the acquisition of the salt used in this study.

Finally, I would like to thank those who have given their support and their encouragement during this project, specifically: Gene Ceguera, Grace Mills, and Patrizia Onnis.

8.0 References

- ABBE, T. B. & MONTGOMERY, D. R. 1996. Large woody debris jams, channel hydraulics and habitat formation in large rivers. *Regulated Rivers- Research & Management*, 12, 201-221.
- ANDERSON, B. G., RUTHERFURD, I. D. & WESTERN, A. W. 2006. An analysis of the influence of riparian vegetation on the propagation of flood waves. *Environmental Modelling & Software*, 21, 1290-1296.
- ARGERICH, A., HAGGERTY, R., MARTÍ, E., SABATER, F. & ZARNETSKE, J. 2011. Quantification of metabolically active transient storage (MATS) in two reaches with contrasting transient storage and ecosystem respiration. *Journal of Geophysical Research: Biogeosciences*, 116.
- BAKER, M. A. & VERVIER, P. 2004. Hydrological variability, organic matter supply and denitrification in the Garonne River ecosystem. *Freshwater Biology*, 49, 181-190.
- BALDIGO, B. P., WARREN, D. R., ERNST, A. G. & MULVIHILL, C. I. 2008. Response of fish populations to natural channel design restoration in streams of the Catskill Mountains, New York. *North American Journal of Fisheries Management*, 28, 954-969.
- BASH, J. S. & RYAN, C. M. 2002. Stream restoration and enhancement projects: is anyone monitoring? *Environmental management*, 29, 877-885.
- BAXTER, C. V. & HAUER, F. R. 2000. Geomorphology, hyporheic exchange, and selection of spawning habitat by bull trout (*Salvelinus confluentus*). *Canadian Journal of Fisheries and Aquatic Sciences*, 57, 1470-1481.
- BECKER, J. F., ENDRENY, T. A. & ROBINSON, J. D. 2013. Natural channel design impacts on reach-scale transient storage. *Ecological Engineering*, 57, 380-392.
- BEECHIE, T. J., SEAR, D. A., OLDEN, J. D., PESS, G. R., BUFFINGTON, J. M., MOIR, H., RONI, P. & POLLOCK, M. M. 2010. Process-based principles for restoring river ecosystems. *BioScience*, 60, 209-222.
- BENCALA, K. E. 1983. Simulation of Solute Transport in a Mountain Pool-and-Riffle Stream with a Kinetic Mass-Transfer Model for Sorption. *Water Resources Research*, 19, 732-738.
- BENCALA, K. E., KENNEDY, V. C., ZELLWEGER, G. W., JACKMAN, A. P. & AVANZINO, R. J. 1984. Interactions of Solutes and Streambed Sediment .1. An Experimental-Analysis of Cation and Anion Transport in a Mountain Stream. *Water Resources Research*, 20, 1797-1803.
- BENCALA, K. E., MCKNIGHT, D. M. & ZELLWEGER, G. W. 1990. Characterization of transport in an acidic and metal-rich mountain stream based on a lithium tracer injection and simulations of transient storage. *Water Resources Research*, 26, 989-1000.
- BERNHARDT, E. S. & PALMER, M. A. 2007. Restoring streams in an urbanizing world. *Freshwater biology*, 52, 738-751.
- BERNHARDT, E. S., PALMER, M. A., ALLAN, J., ALEXANDER, G., BARNAS, K., BROOKS, S., CARR, J., CLAYTON, S., DAHM, C. & FOLLSTAD-SHAH, J. 2005. Synthesizing US river restoration efforts. American Association for the Advancement of Science.
- BINNS, N. A. 2004. Effectiveness of habitat manipulation for wild salmonids in Wyoming streams. *North American Journal of Fisheries Management*, 24, 911-921.

- BOANO, F., CAMPOREALE, C., REVELLI, R. & RIDOLFI, L. 2006. Sinuosity-driven hyporheic exchange in meandering rivers. *Geophysical Research Letters*, 33.
- BOULTON, A. J. 2007. Hyporheic rehabilitation in rivers: restoring vertical connectivity. *Freshwater Biology*, 52, 632-650.
- BOULTON, A. J., DATRY, T., KASAHARA, T., MUTZ, M. & STANFORD, J. A. 2010. Ecology and management of the hyporheic zone: stream-groundwater interactions of running waters and their floodplains. *Journal of the North American Benthological Society*, 29, 26-40.
- BOULTON, A. J., FINDLAY, S., MARMONIER, P., STANLEY, E. H. & VALETT, H. M. 1998. The functional significance of the hyporheic zone in streams and rivers. *Annual Review of Ecology and Systematics*, 29, 59-81.
- BROWN, V. H., EVANS, D. J. & EVANS, I. S. 2011. The glacial geomorphology and surficial geology of the South-West English Lake District. *Journal of Maps*, 7, 221-243.
- BRUNKE, M. & GONSER, T. 1997. The ecological significance of exchange processes between rivers and groundwater. *Freshwater biology*, 37, 1-33.
- BUKAVECKAS, P. A. 2007. Effects of channel restoration on water velocity, transient storage, and nutrient uptake in a channelized stream. *Environmental science & technology*, 41, 1570-1576.
- CARDENAS, M. B., WILSON, J. & ZLOTNIK, V. A. 2004. Impact of heterogeneity, bed forms, and stream curvature on subchannel hyporheic exchange. *Water Resources Research*, 40.
- CASTRO, N. M. & HORNBERGER, G. M. 1991. Surface-Subsurface Water Interactions in an Alluviated Mountain Stream Channel. *Water Resources Research*, 27, 1613-1621.
- CHOI, J., HARVEY, J. W. & CONKLIN, M. H. 2000. Characterizing multiple timescales of stream and storage zone interaction that affect solute fate and transport in streams. *Water Resources Research*, 36, 1511-1518.
- CHURCH, M. & RYDER, J. M. 1972. Paraglacial sedimentation: a consideration of fluvial processes conditioned by glaciation. *Geological Society of America Bulletin*, 83, 3059-3072.
- CONSTANTZ, J. 1998. Interaction between stream temperature, streamflow, and groundwater exchanges in Alpine streams. *Water Resources Research*, 34, 1609-1615.
- COSTANZA, R., D'ARGE, R., DE GROOT, R., FARBER, S., GRASSO, M., HANNON, B., LIMBURG, K., NAEEM, S., O'NEILL, R. V. & PARUELO, J. 1997. The value of the world's ecosystem services and natural capital. *nature*, 387, 253.
- CZERNUSZENKO, W. & ROWINSKI, P. M. 1997. Properties of the dead-zone model of longitudinal dispersion in rivers. *Journal of Hydraulic Research*, 35, 491-504.
- DE SMEDT, F., BREVIS, W. & DEBELS, P. 2005. Analytical solution for solute transport resulting from instantaneous injection in streams with transient storage. *Journal of Hydrology*, 315, 25-39.
- DIXON, S. J., SEAR, D. A., ODoni, N. A., SYKES, T. & LANE, S. N. 2016. The effects of river restoration on catchment scale flood risk and flood hydrology. *Earth Surface Processes and Landforms*, 41, 997-1008.
- DJI 2019. PHANTOM 4 PROSPECS. <https://www.dji.com/uk/phantom-4-pro/info#specs>.

- DUFF, J. H. & TRISKA, F. J. 1990. Denitrification in Sediments from the Hyporheic Zone Adjacent to a Small Forested Stream. *Canadian Journal of Fisheries and Aquatic Sciences*, 47, 1140-1147.
- ELLIOTT, A. H. & BROOKS, N. H. 1997. Transfer of nonsorbing solutes to a streambed with bed forms: Laboratory experiments. *Water Resources Research*, 33, 137-151.
- ENDRENY, T., LAUTZ, L. & SIEGEL, D. 2011. Hyporheic flow path response to hydraulic jumps at river steps: Flume and hydrodynamic models. *Water Resources Research*, 47.
- ENSIGN, S. H. & DOYLE, M. W. 2005. In-channel transient storage and associated nutrient retention: Evidence from experimental manipulations. *Limnology and Oceanography*, 50, 1740-1751.
- FERNALD, A. G., WIGINGTON JR, P. & LANDERS, D. H. 2001. Transient storage and hyporheic flow along the Willamette River, Oregon: Field measurements and model estimates. *Water Resources Research*, 37, 1681-1694.
- FINDLAY, S. 1995. Importance of surface-subsurface exchange in stream ecosystems: The hyporheic zone. *Limnology and oceanography*, 40, 159-164.
- GARIGLIO, F. P., TONINA, D. & LUCE, C. H. 2013. Spatiotemporal variability of hyporheic exchange through a pool-riffle-pool sequence. *Water Resources Research*, 49, 7185-7204.
- GEIST, D. R. 2000. Hyporheic discharge of river water into fall chinook salmon (*Oncorhynchus tshawytscha*) spawning areas in the Hanford Reach, Columbia River. *Canadian Journal of Fisheries and Aquatic Sciences*, 57, 1647-1656.
- GIPPEL, C. J. 1995. Environmental hydraulics of large woody debris in streams and rivers. *Journal of Environmental Engineering*, 121, 388-395.
- GOOSEFF, M. N., WONDZELL, S. M., HAGGERTY, R. & ANDERSON, J. 2003. Comparing transient storage modeling and residence time distribution (RTD) analysis in geomorphically varied reaches in the Lookout Creek basin, Oregon, USA. *Advances in Water Resources*, 26, 925-937.
- HAGGERTY, R., WONDZELL, S. M. & JOHNSON, M. A. 2002. Power-law residence time distribution in the hyporheic zone of a 2nd-order mountain stream. *Geophysical Research Letters*, 29, 18-1-18-4.
- HALL, R. J. O., BERNHARDT, E. S. & LIKENS, G. E. 2002. Relating nutrient uptake with transient storage in forested mountain streams. *Limnology and Oceanography*, 47, 255-265.
- HARVEY, J. W. & BENCALA, K. E. 1993. The effect of streambed topography on surface-subsurface water exchange in mountain catchments. *Water Resources Research*, 29, 89-98.
- HARVEY, J. W. & FULLER, C. C. 1998. Effect of enhanced manganese oxidation in the hyporheic zone on basin-scale geochemical mass balance. *Water Resources Research*, 34, 623-636.
- HARVEY, J. W. & WAGNER, B. J. 2000. Quantifying hydrologic interactions between streams and their subsurface hyporheic zones. *Streams and ground waters*, 3-44.
- HARVEY, J. W., WAGNER, B. J. & BENCALA, K. E. 1996. Evaluating the reliability of the stream tracer approach to characterize stream-subsurface water exchange. *Water Resources Research*, 32, 2441-2451.

- HAYS, J., KRENKEL, P. & SCHNELLE JR, K. 1966. Mass transport mechanisms in open-channel flow, Sanitary and Water Resour. Eng. Tech. Rep. 8, Vanderbilt Univ., Nashville, Tenn.
- HESTER, E. T. & DOYLE, M. W. 2008. In-stream geomorphic structures as drivers of hyporheic exchange. *Water Resources Research*, 44.
- HILL, A. R., LABADIA, C. F. & SANMUGADAS, K. 1998. Hyporheic zone hydrology and nitrogen dynamics in relation to the streambed topography of a N-rich stream. *Biogeochemistry*, 42, 285-310.
- JONES JR, J. B., FISHER, S. G. & GRIMM, N. B. 1995. Nitrification in the hyporheic zone of a desert stream ecosystem. *Journal of the North American Benthological Society*, 14, 249-258.
- KASAHARA, T. & HILL, A. R. 2006. Effects of riffle step restoration on hyporheic zone chemistry in N-rich lowland streams. *Canadian Journal of Fisheries and Aquatic Sciences*, 63, 120-133.
- KASAHARA, T. & WONDZELL, S. M. 2003. Geomorphic controls on hyporheic exchange flow in mountain streams. *Water Resources Research*, 39, SBH 3-1-SBH 3-14.
- KILPATRICK, F. A. & COBB, E. D. 1985. *Measurement of discharge using tracers*, Department of the Interior, US Geological Survey.
- KNUST, A. E. & WARWICK, J. J. 2009. Using a fluctuating tracer to estimate hyporheic exchange in restored and unrestored reaches of the Truckee River, Nevada, USA. *Hydrological Processes: An International Journal*, 23, 1119-1130.
- KONDOLF, G. M., BOULTON, A. J., O'DANIEL, S., POOLE, G. C., RAHEL, F. J., STANLEY, E. H., WOHL, E., BÅNG, Å., CARLSTROM, J. & CRISTONI, C. 2006. Process-based ecological river restoration: visualizing three-dimensional connectivity and dynamic vectors to recover lost linkages. *Ecology & society*, 11, 1-16.
- KONDOLF, G. M., WILLIAMS, J. G., HORNER, T. C. & MILAN, D. Assessing physical quality of spawning habitat. American fisheries society symposium, 2008. 000-000.
- KUPILAS, B. 2017. *Effects of river restoration on ecosystem metabolism and trophic relationships*. Duisburg, Essen, Universität Duisburg-Essen.
- KURTH, A.-M., WEBER, C. & SCHIRMER, M. 2015. How effective is river restoration in re-establishing groundwater–surface water interactions?—A case study. *Hydrology and Earth System Sciences*, 19, 2663-2672.
- LAVE, R. 2009. The controversy over natural channel design: substantive explanations and potential avenues for resolution 1. *JAWRA Journal of the American Water Resources Association*, 45, 1519-1532.
- LIN, Y.-C. & MEDINA JR, M. A. 2003. Incorporating transient storage in conjunctive stream–aquifer modeling. *Advances in Water Resources*, 26, 1001-1019.
- LIU, D., VALYRAKIS, M. & WILLIAMS, R. 2017. Flow hydrodynamics across open channel flows with riparian zones: implications for riverbank stability. *Water*, 9, 720.
- MARTTILA, H., TURUNEN, J., AROVIITA, J., TAMMELA, S., LUHTA, P. L., MUOTKA, T. & KLØVE, B. 2018. Restoration increases transient storages in boreal headwater streams. *River research and applications*, 34, 1278-1285.

- MASON, S. J., MCGLYNN, B. L. & POOLE, G. C. 2012. Hydrologic response to channel reconfiguration on Silver Bow Creek, Montana. *Journal of hydrology*, 438, 125-136.
- MCLACHLAN, M., MACKAY, D. & JONES, P. H. 1990. A conceptual model of organic chemical volatilization at waterfalls. *Environmental science & technology*, 24, 252-257.
- MCMAHON, P. & BÖHLKE, J. 1996. Denitrification and mixing in a stream—Aquifer system: Effects on nitrate loading to surface water. *Journal of hydrology*, 186, 105-128.
- MILLER, S. W., BUDY, P. & SCHMIDT, J. C. 2010. Quantifying macroinvertebrate responses to in-stream habitat restoration: applications of meta-analysis to river restoration. *Restoration Ecology*, 18, 8-19.
- MOORE, R. 2005. Slug injection using salt in solution. *Streamline Watershed Management Bulletin*, 8, 1-6.
- MORRICE, J. A., VALETT, H. M., DAHM, C. N. & CAMPANA, M. E. 1997. Alluvial characteristics, groundwater–surface water exchange and hydrological retention in headwater streams. *Hydrological processes*, 11, 253-267.
- MUELLER PRICE, J., BAKER, D. & BLEDSOE, B. 2016. Effects of passive and structural stream restoration approaches on transient storage and nitrate uptake. *River Research and Applications*, 32, 1542-1554.
- NORDIN JR, C. F. & TROUTMAN, B. M. 1980. Longitudinal dispersion in rivers: The persistence of skewness in observed data. *Water Resources Research*, 16, 123-128.
- PACKMAN, A. I. & MACKAY, J. S. 2003. Interplay of stream-subsurface exchange, clay particle deposition, and streambed evolution. *Water Resources Research*, 39.
- PACKMAN, A. I. & SALEHIN, M. 2003. Relative roles of stream flow and sedimentary conditions in controlling hyporheic exchange. *Hydrobiologia*, 494, 291-297.
- PALMER, M. A., BERNHARDT, E., ALLAN, J., LAKE, P. S., ALEXANDER, G., BROOKS, S., CARR, J., CLAYTON, S., DAHM, C. & FOLLSTAD SHAH, J. 2005. Standards for ecologically successful river restoration. *Journal of applied ecology*, 42, 208-217.
- PALMER, M. A., ZEDLER, J. B. & FALK, D. A. 2016. *Foundations of restoration ecology*, Island Press.
- PESS, G. R., MORLEY, S. A., HALL, J. L. & TIMM, R. K. 2005. Monitoring floodplain restoration. *Monitoring stream and watershed restoration. American Fisheries Society, Bethesda, Maryland*, 127-166.
- RANA, S. M., SCOTT, D. T. & HESTER, E. T. 2017. Effects of in-stream structures and channel flow rate variation on transient storage. *Journal of hydrology*, 548, 157-169.
- RILEY, S. C. & FAUSCH, K. D. 1995. Trout population response to habitat enhancement in six northern Colorado streams. *Canadian Journal of Fisheries and Aquatic Sciences*, 52, 34-53.
- ROBERTS, B. J., MULHOLLAND, P. J. & HOUSER, J. N. 2007. Effects of upland disturbance and instream restoration on hydrodynamics and ammonium uptake in headwater streams. *Journal of the North American Benthological Society*, 26, 38-53.

- RONI, P., HANSON, K. & BEECHIE, T. 2008. Global review of the physical and biological effectiveness of stream habitat rehabilitation techniques. *North American Journal of Fisheries Management*, 28, 856-890.
- RUNKEL, R. L. 1998. One-dimensional transport with inflow and storage (OTIS): A solute transport model for streams and rivers. *Water-Resources Investigations Report*, 98, 4018.
- RUNKEL, R. L. 2002. A new metric for determining the importance of transient storage. *Journal of the North American Benthological Society*, 21, 529-543.
- RUNKEL, R. L. & CHAPRA, S. C. 1993. An efficient numerical solution of the transient storage equations for solute transport in small streams. *Water Resources Research*, 29, 211-215.
- RUNKEL, R. L., MCKNIGHT, D. M. & RAJARAM, H. 2003. Modeling hyporheic zone processes. *Advances in Water Resources*, 26, 901-905.
- SHOLTES, J. S. & DOYLE, M. W. 2010. Effect of channel restoration on flood wave attenuation. *Journal of Hydraulic Engineering*, 137, 196-208.
- STOFLETH, J. M., SHIELDS JR, F. D. & FOX, G. A. 2008. Hyporheic and total transient storage in small, sand-bed streams. *Hydrological Processes: An International Journal*, 22, 1885-1894.
- THACKSTON, E. L. & SCHNELLE, K. B. 1970. Predicting effects of dead zones on stream mixing. *Journal of the Sanitary Engineering Division*, 96, 319-331.
- THORNE, C. R. 1998. *Stream reconnaissance handbook: geomorphological investigation and analysis of river channels*, John Wiley & Sons Ltd.
- TOCKNER, K. & STANFORD, J. A. 2002. Riverine flood plains: present state and future trends. *Environmental conservation*, 29, 308-330.
- WAGNER, B. J. & HARVEY, J. W. 1997. Experimental design for estimating parameters of rate-limited mass transfer: Analysis of stream tracer studies. *Water Resources Research*, 33, 1731-1741.
- WARD, A. S., MORGAN, J. A., WHITE, J. R. & ROYER, T. V. 2018. Streambed restoration to remove fine sediment alters reach-scale transient storage in a low-gradient fifth-order river, Indiana, USA. *Hydrological processes*, 32, 1786-1800.
- WEIGELHOFER, G. 2017. The potential of agricultural headwater streams to retain soluble reactive phosphorus. *Hydrobiologia*, 793, 149-160.
- WENTWORTH, C. K. 1922. A scale of grade and class terms for clastic sediments. *The journal of geology*, 30, 377-392.
- WENZEL, R., REINHARDT-IMJELA, C., SCHULTE, A. & BÖLSCHER, J. 2014. The potential of in-channel large woody debris in transforming discharge hydrographs in headwater areas (Ore Mountains, Southeastern Germany). *Ecological engineering*, 71, 1-9.
- WILLIAMS, R., BRASINGTON, J., VERICAT, D. & HICKS, D. 2014. Hyperscale terrain modelling of braided rivers: fusing mobile terrestrial laser scanning and optical bathymetric mapping. *Earth Surface Processes and Landforms*, 39, 167-183.
- WOHL, E., ANGERMEIER, P. L., BLEDSOE, B., KONDOLF, G. M., MACDONNELL, L., MERRITT, D. M., PALMER, M. A., POFF, N. L. & TARBOTON, D. 2005. River restoration. *Water Resources Research*, 41.
- WOHL, E., LANE, S. N. & WILCOX, A. C. 2015. The science and practice of river restoration. *Water Resources Research*, 51, 5974-5997.

- WONDZELL, S. M. 2006. Effect of morphology and discharge on hyporheic exchange flows in two small streams in the Cascade Mountains of Oregon, USA. *Hydrological Processes: An International Journal*, 20, 267-287.
- WONDZELL, S. M. & SWANSON, F. J. 1999. Floods, channel change, and the hyporheic zone. *Water Resources Research*, 35, 555-567.
- WOOLSEY, S., CAPELLI, F., GONSER, T., HOEHN, E., HOSTMANN, M., JUNKER, B., PAETZOLD, A., ROULIER, C., SCHWEIZER, S. & TIEGS, S. D. 2007. A strategy to assess river restoration success. *Freshwater Biology*, 52, 752-769.
- WÖRMAN, A., PACKMAN, A. I., JOHANSSON, H. & JONSSON, K. 2002. Effect of flow-induced exchange in hyporheic zones on longitudinal transport of solutes in streams and rivers. *Water Resources Research*, 38, 2-1-2-15.

9.0 Appendix

In order to match the observed and simulated breakthrough curves onto each other, the channel parameters must be manually changed within the OTIS model. Increasing the dispersion coefficient (D) would lower the maximum point of the estimated breakthrough, while decreasing D would increase the maximum point. Increasing the main channel cross-sectional area parameter (A) moves the maximum point of the simulated curve to the right while decreasing A moves the maximum point to the left.

Tests of Normality for OTIS Parameters 2016 and 2017			
	Shapiro-Wilk		
	Statistic	df	Sig.
D	0.903	8	0.310
A	0.904	8	0.316
A2	0.908	8	0.341
α	0.949	8	0.700
V	0.948	8	0.686

Table 8: Sig. value is greater than 0.05, so the data is normal

Test Statistics for OTIS Parameters 2016 and 2017					
	D	A	A2	Alpha	V
Mann-Whitney U	3.000	8.000	5.000	4.000	4.000
Sig.	0.149	1.000	0.386	0.248	0.248

Table 9: There is no significant difference between the OTIS parameters 2016 and 2017.

Tests of Normality for OTIS Metrics 2016 and 2017			
	Shapiro-Wilk		
	Statistic	df	Sig.
Dal	0.885	9	0.175
F200med	0.923	9	0.414
TimeStor	0.595	9	0.000
TranStor	0.946	9	0.645
Ls	0.917	9	0.369
qs	0.953	9	0.718
Rh	0.749	9	0.005

Table 10: Table showing results of tests for normality. Sig values above 0.005 are normal and values below are non-normal, indicating TimeStor and Rh metrics are non-normal whereas the other metrics or normal.

Test Statistics for OTIS Metrics 2016 and 2017							
	Dal	Fmed@200	TimeStor	Ls	TranStor	qs	Rh
Mann-Whitney U	7.000	3.000	8.000	4.000	4.000	3.000	5.000
Asymp. Sig.	0.773	0.149	1.000	0.248	0.248	0.149	0.386

Table 11: There is no significant difference between the OTIS metrics 2016 and 2017.

Tests of Normality			
	Shapiro-Wilk		
	Statistic	Degrees of Freedom	Sig.
Bars Area (2016)	0.903	19	0.055
Bars Area (2017)	0.907	19	0.066

Table 12: Sig. value is greater than 0.05, so the data is normal

Tests of Normality			
	Shapiro-Wilk		
	Statistic	Degrees of Freedom	Sig.
Pools Area (2016)	0.818	9	0.032
Pools Area (2017)	0.688	9	0.001

Table 13: Sig. value is smaller than 0.05, so the data is non-normal.

Tests of Normality			
	Shapiro-Wilk		
	Statistic	Degrees of Freedom	Sig.
Riffles Area (2016)	0.825	10	0.029
Riffles Area (2017)	0.937	10	0.524

Table 14: Sig. value is smaller than 0.05 for the 2016 data, but it is greater for the 2017 data. The 2016 data is normal whereas the 2017 data is non-normal.

T Test						
	T Statistic	Degrees of Freedom	Sig.	Mean Difference	95% Confidence Interval of the Difference	
					Lower	Upper
Bars Area (2016)	7.22	18	0.000001	66.76	47.33	86.20
Bars Area (2017)	5.65	19	0.000019	75.32	47.40	103.24

Table 15: There was a significant increase in the area of bars (1256m² to 1506m²) in reaches from 2016 to 2017.

Mann-Whitney U	
	Pools Area
Mann-Whitney U	61.000
Sig.	0.926

Table 16: There was no significant increase in the area of pools (158m² to 262m²) in reaches from 2016 to 2017. However since the Sig Value is close to 0.05 it is possible that error will overlap with this 0.05 threshold

Mann-Whitney U	
	Riffles Area
Mann-Whitney U	45.000
Sig.	0.346

Table 17: There was no significant increase in the area of riffles (350m² to 481m²) in reaches from 2016 to 2017.

		River Reach Survey							
		<u>SB1 Right Bank</u>	<u>SB1 Left Bank</u>	<u>SB2 Right Bank</u>	<u>SB2 Left Bank</u>	<u>SB3 Right Bank</u>	<u>SB3 Left Bank</u>	<u>SB4 Right Bank</u>	<u>SB4 Left Bank</u>
Bank Characteristics	Type	Composite	Cohesive	Cohesive	Cohesive	Composite	Cohesive	Cohesive	Composite
	Bank Materials	Silt/Clay/Sand/Cobbles	Silt/Clay/Sand	Silt/Clay	Silt/Clay	Silt/Clay/Sand/Cobbles/Boulders	Silt/Clay	Silt/Clay	Silt/Clay/Sand/Cobbles/Boulders
	Average Bank Height	1m	1m	0.7m	0.7m	1.5m	1m	1m	1m
	Average Bank Slope Angle	60 Degrees	45 Degrees	90 Degrees	30 Degrees	25 Degrees	20 Degrees	90 Degrees	90 Degrees

Bank-Face Vegetation	Vegetation	Grass and Flora	Grass and Flora	Grass and Flora	Grass, Flora and Reeds	Grass and Flora, Trees	Grass and Flora, Saplings	Grass and Flora	Grass and Flora
	Tree Types	None	None	None	None	Deciduous	Deciduous	None	None
	Vegetation Density	Dense Continuous	Dense Continuous	Dense Continuous	Dense Continuous	Dense Continuous, Sparse Trees	Dense Continuous, Sparse Trees	Dense Continuous	Dense Continuous
	Vegetation Location	Upper Bank	Upper Bank	Upper Bank	Upper, Mid, Lower Bank	Upper Bank	Upper Bank	Upper Bank	Upper Bank
	Vegetation Height	Short	Short	Medium	Short	Medium	Medium	Medium	Medium

Bank Erosion	Erosion Location	Outside Meander	Inside Meander	General	General	Outside Meander	Inside Meander	General	General
	Present Status	Eroding (Dormant)	Eroding (Dormant)	Eroding (Active)	No Erosion (Intact)	Eroding (Dormant)	No Erosion (Intact)	No Erosion (Intact)	No Erosion (Intact)
	Severity	Mild	Insignificant	Insignificant	Insignificant	Significant	Insignificant	Insignificant	Insignificant
	Extent	Local	Local	Local	None	General	Local	None	None
	Processes	Parallel Flow	Parallel Flow	Parallel Flow	Parallel Flow	Parallel and Impinging Flow	Parallel Flow	Parallel Flow	Parallel Flow

Table 18: 2018 River reach survey (conducted in 2018) based on the stream reconnaissance handbook (Thorne, 1998). The left bank is true left and the right bank is true right.